AFCRL - 64-855

SEISMIC ARRAYS FOR THE DETECTION OF NUCLEAR EXPLOSIONS

E. A. Robinson

Massachusetts Institute of Technology
Cambridge 39, Massachusetts

Scientific Report No. 8 of Contract
AF 19(604) 7[illegible]8
S. M. Simpson, Director
June 30, 1964
Project 8652
Task 865203

Prepared for

AIR FORCE CAMBRIDGE RESEARCH LABORATORIES
OFFICE OF AEROSPACE RESEARCH
UNITED STATES AIR FORCE
BEDFORD, MASSACHUSETTS

WORK SPONSORED BY ADVANCED RESEARCH PROJECTS AGENCY
PROJECT VELA-UNIFORM
ARPA Order No. 180-61, Amendment 2

BLANK PAGE

AFCRL - 64-855

SEISMIC ARRAYS FOR THE DETECTION OF NUCLEAR EXPLOSIONS

E. A. Robinson

Massachusetts Institute of Technology
Cambridge 39, Massachusetts

Scientific Report No. 8 of Contract
AF 19(604) 7378
S. M. Simpson, Director
June 30, 1964
Project 8652
Task 865203

Prepared for

AIR FORCE CAMBRIDGE RESEARCH LABORATORIES
OFFICE OF AEROSPACE RESEARCH
UNITED STATES AIR FORCE
BEDFORD, MASSACHUSETTS

WORK SPONSORED BY ADVANCED RESEARCH PROJECTS AGENCY

PROJECT VELA-UNIFORM
ARPA Order No. 180-61, Amendment 2

Requests for additional copies by Agencies of the Department of Defense, their contractors, and other Government agencies should be directed to the:

DEFENSE DOCUMENTATION CENTER (DDC)
CAMERON STATION
ALEXANDRIA, VIRGINIA 22314

Department of Defense contractors must be established for DDC services or have their 'need-to-know' certified by the cognizant military agency of their project or contract.

All other persons and organizations should apply to the:

U. S. DEPARTMENT OF COMMERCE
OFFICE OF TECHNICAL SERVICES
WASHINGTON D. C. 20230

ABSTRACT

Seismic arrays are multichannel sensor patterns immersed in a multi-dimensional signal-noise field and the analytic problem is hence analogous to that of radar antennas. The subject is thus opened first by a review of antenna theory, considering questions of aperture width, antenna resolution, and of optimum design criteria, and secondly by a review of spectral theory, including special examination of the Ross "time gates". The general optimization problem for multichannel data leads to large systems of normal equations of Toeplitz form (as presented in previous reports) which require recursion solution techniques to be computationally feasible. Such techniques are elaborated here in terms of polynomials orthogonal on the unit circle. The specific seismic array problem is then considered in terms of plane-wave-front signal and noise contributions plus incoherent noise, and details of the "velocity filtering" method are presented. All practical array filtering rests ultimately on empirical measurements of signal and noise properties, especially of spectral behavior. Spectral estimation from finite array measurements is the final question considered, including relations between continuous and discrete aperture functions, and the tabulation of aperture functions with their windows.

TABLE OF CONTENTS

THIS
PAGE
IS
MISSING
IN
ORIGINAL
DOCUMENT

SEISMIC ARRAYS FOR THE DETECTION OF NUCLEAR EXPLOSIONS

Enders A. Robinson

May 1964

1. REVIEW OF ANTENNA THEORY

Arrays of detectors have velocity discrimination properties and hence directional sensitivity. In the first part of this treatment we would like to review the general theory of the directional properties of antennas in order to bring out some of the design problems for arrays of specified directivity.

An antenna may be viewed as a spatial filter, and so has a bandwidth that is determinded by the aperture extent; therefore, it will reproduce only a finite number of the space harmonics representing a desired spatial pattern. From this standpoint, the antenna resolution is limited by the highest space harmonic within the bandwidth of the spatial filter; this bandwidth in turn is determined by the aperture size. Nevertheless, this well-known limitation on antenna resolution may be overcome by the use of correlation type processing of the antenna signals. The spatial-frequency bandwidth, and hence the angular resolution, of an antenna system thus depends not only on the aperture extent but also on the time-frequency bandwidth of the received signal. This is to be expected, since the aperture extent is only uniquely defined in terms of wavelengths and hence the signal bandwidth should play a part in determining the spatial filter characteristics.

For example, let us look at a radar antenna. Suppose that a linear antenna is constructed so that the radiated

electric field across its face is sinusoidal in time with an amplitude and phase depending on position according to the complex-valued function of position $A_a(x)$. The superposition of the contributions along the antenna give the antenna pattern. By examining the figure, we see that the distance traveled by the incremental wave from the position $(x, x+dx)$ varies with the position x.

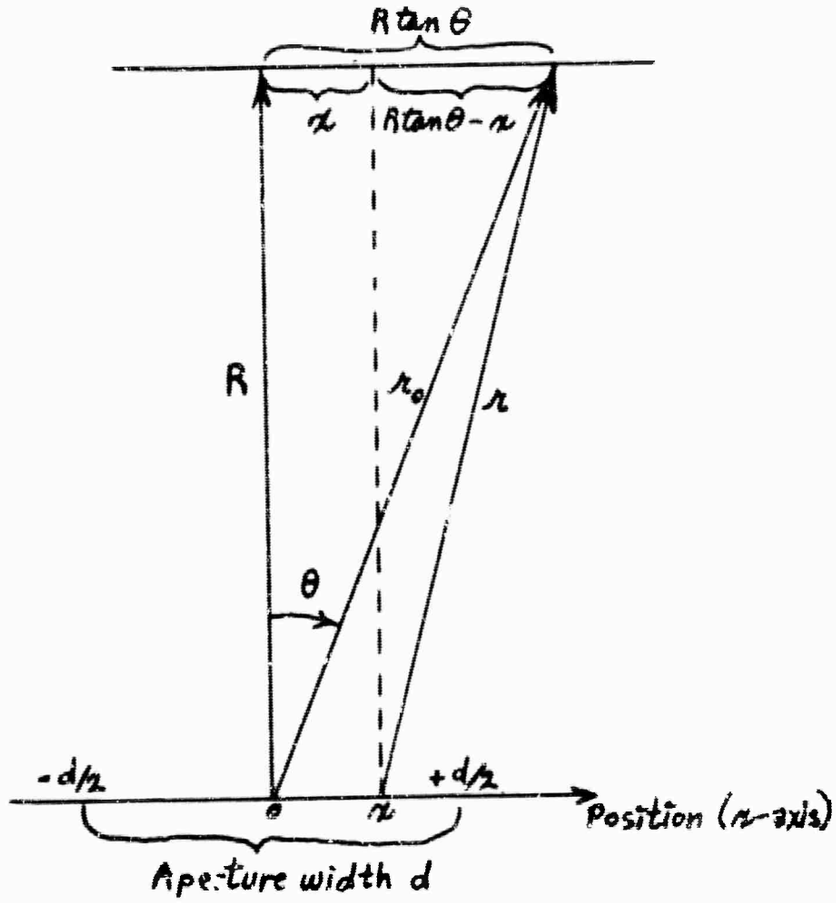

Figure 1. Radar antenna geometry

We have:

$$r_0 = \sqrt{R^2 + (R\tan\theta)^2} = R\sqrt{1+\tan^2\theta} \approx R\left[1+\frac{\tan^2\theta}{2}\right]$$

$$r = \sqrt{R^2 + (R\tan\theta - x)^2} \approx R\left[1+\frac{(R\tan\theta - x)^2}{2R^2}\right].$$

If $A_0(x) = M(x)\, e^{i\phi(x)}$, then the sine wave received from the position $(x, x+dx)$ is

$$M \cos\left[\omega_0\left(t-\frac{r}{c}\right)+\phi\right] dx$$
$$= M \cos\left[\omega_0 t + \phi - \frac{2\pi r}{\lambda}\right] dx$$

where

$$\frac{2\pi c}{\omega} = \lambda \qquad (c = \text{velocity of light}).$$

Let us use a reference phase of $\frac{2\pi r_0}{\lambda}$ when at a distance r_0 .

Then the received signal can be written as

$$M \cos\left[\omega_0 t + \phi + \frac{2\pi}{\lambda}(r_0 - r)\right] dx.$$

We will now make the approximation

$$r_0 - r \approx R\left[1+\frac{\tan^2\theta}{2}\right] - R\left[1+\frac{(R\tan\theta - x)^2}{2R^2}\right]$$
$$\approx x\tan\theta - \frac{x^2}{2R}$$

which is good for small θ and large R . By "far field" we mean that R is so large that $\frac{x^2}{2R}$ can be neglected; the important criterion is for

$$\frac{\left(\frac{d}{2}\right)^2}{2R} \ll \lambda$$

where d is the aperture width. Also we shall let $\tan\theta \approx \theta$, so

$$r_0 - r \approx x \tan\theta \approx x\theta.$$

Hence the received signal may be written

$$M \cos[\omega t + \phi + \tfrac{2\pi}{\lambda} x\theta]\, dx.$$

Adding sine waves of the same frequency, the amplitude and phase of the total signal received at an angle θ is given by

$$a(\theta) = \int_{-\frac{d}{2}}^{\frac{d}{2}} M(x)\, e^{i\phi(x)}\, e^{i\frac{2\pi}{\lambda}x\theta}\, dx.$$

Letting

$$\omega = \frac{2\pi x}{\lambda} \qquad \text{and} \qquad \lambda A_0\left(\frac{\lambda\omega}{2\pi}\right) \equiv A(\omega)$$

we have

$$a(\theta) = \frac{1}{2\pi} \int_{-\frac{\pi d}{\lambda}}^{\frac{\pi d}{\lambda}} A(\omega)\, e^{i\omega\theta}\, d\omega.$$

Thus we see that the antenna pattern $a(\theta)$ is the inverse Fourier transform of the illumination function $A(\omega)$. Because of the finite aperture width, that is,

$$A(\omega) = 0 \qquad \text{for} \quad |\omega| > \frac{\pi d}{\lambda},$$

the antenna pattern is the Fourier transform of a band-limited function. Thus a narrow beam width would require a wide aperture width d of the antenna.

There are various ways to measure the beam width of an antenna pattern, $a(\theta)$. Suppose that $a(\theta)$ is real. Then

$$\sigma^2 = \frac{\int_{-\infty}^{\infty} (\theta - \bar{\theta})^2 a(\theta)\, d\theta}{\int_{-\infty}^{\infty} a(\theta)\, d\theta}$$

(where $\bar{\theta} = \int_{-\infty}^{\infty} \theta\, a(\theta)\, d\theta \Big/ \int_{-\infty}^{\infty} a(\theta)\, d\theta$) might be small not because $a(\theta)$ is concentrated around $\bar{\theta}$ on the θ-axis but because the contributions to the numerator for $a>0$ might be cancelled by the contributions for $a<0$. Thus we see that it is $|d\theta|$ that is involved in our intuitive notion of the spread of $a(\theta)$ on the θ-axis. Also $|a(\theta)|$ allows us to consider complex $a(\theta)$ as well as real $a(\theta)$. Now for analytic reasons, it is much easier to work with $|a(\theta)|^2$ instead of $|a(\theta)|$; as far as spread on the θ-axis is concerned, $|a(\theta)|^2$ is as satisfactory as $|a(\theta)|$, although obviously there are quantitative differences depending upon which we use.

Thus the beam width of an antenna pattern $a(\theta)$ may be measured by the quantity

$$\alpha^2 = \frac{\int_{-\infty}^{\infty} (\theta - \bar{\theta})^2 |a(\theta)|^2 d\theta}{\int_{-\infty}^{\infty} \theta |a(\theta)|^2 d\theta}$$

where

$$\bar{\theta} = \frac{\int_{-\infty}^{\infty} \theta \, |a(\theta)|^2 d\theta}{\int_{-\infty}^{\infty} |a(\theta)|^2 d\theta} .$$

It is always worthwhile to consider other measures for spread along the θ-axis. Another measure may be referred to the equivalent rectangle; specifically, the measure ρ is the width of a rectangle having the same area as $|a(\theta)|^2$ and having the same peak value as $|a(\theta)|^2$. If we let $|a(\theta_0)|^2$ denote the peak value of $|a(\theta)|^2$, then

$$\rho = \frac{\int_{-\infty}^{\infty} |a(\theta)|^2 d\theta}{|a(\theta_0)|^2}$$

This measure is not good for antenna patterns for which $|a(\theta)|^2$ is not reasonably block-shaped.

Let us now derive expressions for α and ρ in terms of the illumination function $A(\omega)$. Because we can choose our origin of coordinates as we like, we may assume that $\bar{\theta}$ and θ_0 are equal to zero. This involves replacing $a(\theta)$ by $a(\theta - \bar{\theta})$ or $a(\theta - \theta_0)$ as the case may be; in turn, the illumination function is modified by a linear phase term $e^{-i\omega\bar{\theta}}$ or $e^{-i\omega\theta_0}$ respectively.

Parseval's theorem states that

$$\int_{-\infty}^{\infty} |a(\theta)|^2 d\theta = \frac{1}{2\pi} \int_{-\infty}^{\infty} |A(\omega)|^2 d\omega ,$$

and also we have

$$a(\theta) = \frac{1}{2\pi}\int_{-\infty}^{\infty} e^{i\omega\theta} A(\omega)\, d\omega = \frac{1}{2\pi}\int_{-\infty}^{\infty} A(\omega)\, d\omega .$$

Hence the measure of spread, ρ , is

$$\rho = \frac{\frac{1}{2\pi}\int_{-\infty}^{\infty} |A(\omega)|^2 d\omega}{\left|\frac{1}{2\pi}\int_{-\infty}^{\infty} A(\omega)\, d\omega\right|^2} = \frac{2\pi\int_{-\infty}^{\infty} |A(\omega)|^2 d\omega}{\left|\int_{-\infty}^{\infty} A(\omega)\, d\omega\right|^2} ,$$

the width of the equivalent rectangle. To obtain a formula for α^2 in terms of $A(\omega)$, we must use two applications of Parseval's theorem, one for $a(\theta)$ and the other for $\theta\, a(\theta)$. Because

$$A(\omega) = \int_{-\infty}^{\infty} a(\theta)\, e^{-i\omega\theta}\, d\theta$$

we have

$$A'(\omega) = -i\int_{-\infty}^{\infty} \theta\, a(\theta)\, e^{-i\omega\theta}\, d\theta .$$

That is

$$i A'(\omega) \longleftrightarrow \theta\, a(\theta)$$

is a Fourier transform pair. Thus, using Parseval's theorem for this pair, we have

$$\int_{-\infty}^{\infty} |\theta\, a(\theta)|^2 d\theta = \frac{1}{2\pi}\int_{-\infty}^{\infty} |iA'(\omega)|^2 d\omega = \frac{1}{2\pi}\int_{-\infty}^{\infty} |A'(\omega)|^2 d\omega.$$

Thus the measure of spread, α^2 , is

$$\alpha^2 = \frac{\int_{-\infty}^{\infty} \theta^2 |a(\theta)|^2 d\theta}{\int_{-\infty}^{\infty} |a(\theta)|^2 d\theta} = \frac{\int_{-\infty}^{\infty} |A'(\omega)|^2 d\omega}{\int_{-\infty}^{\infty} |A(\omega)|^2 d\omega}.$$

These formulas for ρ and α^2 allow us to study the dependence of beam width upon features of the illumination function $A(\omega)$.

The illumination function may be written

$$A(\omega) = M(\omega) e^{i\phi(\omega)}$$

where $M(\omega)$ is the magnitude and $\phi(\omega)$ is the phase. We now want to show that, for any fixed magnitude function $M(\omega)$, the phase function $\phi(\omega)$ that minimizes the beam width is a constant (or linear function of ω). Since, under the assumed conditions,

$$\rho = \frac{2\pi \int_{-\infty}^{\infty} |A|^2 d\omega}{\left| \int_{-\infty}^{\infty} A\, d\omega \right|^2} = \frac{2\pi \int_{-\infty}^{\infty} M^2 d\omega}{\left| \int_{-\infty}^{\infty} M e^{i\phi} d\omega \right|^2}$$

where M is fixed, we want to choose ϕ to maximize the denominator. Because

$$\left| \int_{-\infty}^{\infty} M e^{i\phi} d\omega \right| \leq \int_{-\infty}^{\infty} |M e^{i\phi}| \, d\omega = \int_{-\infty}^{\infty} M \, d\omega$$

we see that we get equality only if ϕ is a constant, which proves our assertion. Let us now look at the beam width α^2. Because

$$A'(\omega) = M'(\omega) e^{i\phi(\omega)} + M(\omega) i \phi'(\omega) e^{i\phi(\omega)},$$

we have

$$\alpha^2 = \frac{\int_{-\infty}^{\infty} |M' + iM\phi'|^2 d\omega}{\int_{-\infty}^{\infty} M^2 d\omega}$$

because the factor $e^{i\phi}$ has no effect on $|A'|^2$.

Because M' and $M\phi'$ are real, the only way to minimize $|M' + iM\phi'|^2 = (M')^2 + (M\phi')^2$ for fixed M is to make $\phi' = 0$, which means that ϕ would be a constant. Nevertheless, since we only need to make $M\phi' = 0$, the points at which $M(\omega) = 0$ need not be points for which $\phi'(\omega) = 0$. Thus, suppose $M'(\omega)$ exists except possibly at isolated points where $M(\omega) = 0$ and at

such points let $M(\omega)$ be at least continuous. Then any $\phi(\omega)$ that is constant between adjacent zeros of H minimizes α^2. As usual, any linear phase $i\omega\bar{\theta}$ can be subtracted from the minimizing $\phi(\omega)$ without changing the beam width α^2 because the effect is only to translate $Q(\theta)$ along the θ-axis.

Suppose that the antenna pattern $Q(\theta)$ is real. Because

$$A(\omega) = \int_{-\infty}^{\infty} Q(\omega)\, e^{-i\omega\theta}\, d\theta ,$$

we have

$$\overline{A(\omega)} = \int_{-\infty}^{\infty} Q(\theta)\, e^{i\omega\theta}\, d\theta = \int_{-\infty}^{\infty} Q(\theta)\, e^{-i(-\omega)\theta}\, d\theta$$
$$= A(-\omega) ,$$

or

$$M(\omega)\, e^{-i\phi(\omega)} = M(-\omega)\, e^{i\phi(-\omega)} .$$

Thus the phase condition for minimum beam width, namely $\phi(\omega) =$ constant, requires that $\phi(\omega) = 0$, and $M(\omega) = M(-\omega)$ so that $A(\omega) = M(\omega)$ is a real even function. In turn, the antenna pattern $Q(\theta)$ is an even function.

Let us now look at the effects of the magnitude $M(\omega)$ of the illumination function on the beam width of the antenna pattern $Q(\omega)$. Because the beam width can be made arbitrarily small if the bandwidth of $M(\omega)$ is made large enough, the appropriate problem is to minimize beam width when the aperture bandwidth is limited. Thus we need a measure of the spread of the illumination function $A(\omega)$ on

the ω-axis to provide a numerical measure of bandwidth. One such notion of bandwidth is the radius of gyration

$$\beta^2 = \frac{\int_{-\infty}^{\infty} \omega^2 |A(\omega)|^2 \, d\omega}{\int_{-\infty}^{\infty} |A(\omega)|^2 \, d\omega}$$

where we assume that

$$\bar{\omega} = \int_{-\infty}^{\infty} \omega |A(\omega)|^2 \, d\omega = 0.$$

This last restriction only amounts to a translation of $A(\omega)$ by an amount $\bar{\omega}$, corresponding to multiplying $a(b)$ by $e^{i\bar{\omega}\theta}$, which has no effect on α (or β). Another notion of bandwidth is the natural one for antennas with finite aperture width; here it is assumed that $H(\omega) = 0$ outside of an interval (corresponding to the aperture) on the ω-axis. We define k as half the length of the interval; in terms of our previous notation

$$A(\omega) = 0 \quad \text{for} \quad |\omega| > k = \frac{\pi d}{\lambda}$$

where d = aperture width and $\lambda = \frac{2\pi c}{\omega}$ (where c = velocity of light).

We now wish to show that broad illumination bandwidth gives a narrow beam width (that is, a good antenna resolution).

From the definitions of α^2 and β^2, we have

$$\alpha^2\beta^2 = \frac{\int_{-\infty}^{\infty}|A'|^2 d\omega}{\int_{-\infty}^{\infty}|A|^2 d\omega}\,\frac{\int_{-\infty}^{\infty}\omega^2|A|^2 d\omega}{\int_{-\infty}^{\infty}|A|^2 d\omega},$$

By use of the Schwarz inequality, it follows that

$$\left|\int_{-\infty}^{\infty}\omega AA' d\omega\right|^2 \leq \int_{-\infty}^{\infty}|\omega A|^2 d\omega \cdot \int_{-\infty}^{\infty}|A'|^2 d\omega$$

so

$$\frac{\left|\int_{-\infty}^{\infty}\omega AA' d\omega\right|^2}{\left(\int_{-\infty}^{\infty}|A|^2 d\omega\right)^2} \leq \alpha^2\beta^2$$

We assume that the phase $\phi(\omega)=0$ in

$$A(\omega) = M(\omega)\, e^{i\phi(\omega)}$$

so that

$$A(\omega) = M(\omega)$$

is real. Hence we see that

$$AA' = \frac{1}{2}\frac{dA^2}{d\omega}$$

thereby giving

$$\left|\int_{-\infty}^{\infty}\omega AA' d\omega\right|^2 = \frac{1}{4}\left|\int_{-\infty}^{\infty}\omega\left(\frac{dA^2}{d\omega}\right) d\omega\right|^2$$

for the numerator of the above expression. If we integrate by parts, we therefore obtain

$$\frac{1}{4}\left| \omega A^2 \Big]_{-\infty}^{\infty} - \int_{-\infty}^{\infty} H^2 d\omega \right|^2$$

for the numerator, and since $\omega A^2 \to 0$ as $|\omega| \to \infty$, this expression reduces to

$$\frac{1}{4}\left| -\int_{-\infty}^{\infty} A^2 \, d\omega \right|^2 .$$

Hence

$$\frac{1}{4} \leq \alpha^2 \beta^2$$

or

$$\alpha\beta \geq \frac{1}{2} ,$$

Which is the fundamental expression relating the measure α^2 of the beam width (or antenna resolution) and the measure β^2 of the illumination bandwidth (or aperture width). Thus if we wish to narrow the beam width of the antenna pattern it is necessary to broaden the band width of the antenna illumination.

The lower bound of $\frac{1}{2}$ for $\alpha\beta$ is actually obtained for the Gaussian-shaped illumination function

$$A(\omega) = C e^{-\frac{\omega^2}{4\beta^2}}$$

(where C = a positive constant)

which yields the antenna pattern (which is also Gaussian-shaped)

$$\alpha(\theta) = C\, e^{-\frac{\theta^2}{4\beta^2}}$$ (where C = a positive constant).

Nevertheless, there is no upper bound for $\alpha\beta$.

A similar result to $\alpha\beta \geq \frac{1}{2}$ can be obtained by using the width of the equivalent rectangular ρ to measure beam width of the antenna pattern $\alpha(\theta)$ and using finite aperture width to measure the bandwidth k of the illumination $A(\omega)$. We suppose that

$$A(\omega) = 0 \qquad \text{for} \quad |\omega| > k .$$

Hence the width of the equivalent rectangle is

$$\rho = \frac{2\pi \int_{-k}^{k} |A|^2 d\omega}{\left| \int_{-k}^{k} A\, d\omega \right|^2}$$

The integrand of the denominator is A , which we may write as $1 \cdot A$ in order to apply the Schwarz inequality. Thus we have

$$\left| \int_{-k}^{k} (A \cdot 1)\, d\omega \right|^2 \leq \int_{-k}^{k} |A|^2 d\omega \cdot \int_{-k}^{k} d\omega = 2k \int_{-k}^{k} |A|^2 d\omega$$

so

$$\rho \geq \frac{2\pi \int_{-k}^{k} |A|^2 d\omega}{2k \int_{-k}^{k} |A|^2 d\omega} = \frac{2\pi}{2k} = \frac{\pi}{k}.$$

Therefore the following inequality is satisfied:

$$k\rho \geq \pi.$$

The equality is satisfied if and only if the illumination is a constant for $|\omega| < k$, in which case the antenna pattern is

$$a(\theta) = C \frac{\sin k\theta}{\theta} \qquad \text{(where } C \text{ = a constant)}$$

In view that

$$k\rho = \pi$$

for a constant illumination function over the finite aperture, that is, for

$$H(\omega) = \begin{cases} \text{constant} & \text{for } |\omega| \leq k \\ 0 & \text{for } |\omega| \geq k \end{cases}$$

it follows that this illumination is optimum in the sense of giving the smallest possible equivalent-rectangle width for a given aperture size. Nevertheless, if we measure the beam width (i.e., antenna resolution) in terms of radius of gyration instead of in terms of equivalent rectangle, we obtain a different result for the optimum illumination function for a finite aperture.

The finite aperture restriction is that the illumination function satisfies the condition

$$A(\omega) = 0 \qquad \text{for} \quad |\omega| > k.$$

The result that we seek is the shape of

$$A(\omega) \qquad \text{for} \quad |\omega| \leq k$$

such that the product

$$\alpha k$$

is a minimum. To minimize α, A will have a constant phase that we can take to be zero, so

$$A(\omega) = M(\omega)$$

is real. We recall that

$$\alpha^2 = \frac{\int_{-\infty}^{\infty} |A'|^2 d\omega}{\int_{-\infty}^{\infty} |A|^2 d\omega} = \frac{\int_{-\infty}^{\infty} (A')^2 d\omega}{\int_{-\infty}^{\infty} A^2 d\omega}$$

Thus we wish to minimize

$$\int_{-\infty}^{\infty} (A')^2 d\omega = \int_{-k}^{k} (A')^2 d\omega$$

with the constraint

$$\int_{-\infty}^{\infty} A^2 \, d\omega = \int_{-k}^{k} A^2 \, d\omega = \text{constant.}$$

Using the calculus of variations, the solution comes out to be

$$A(\omega) = C \cos\left(\frac{\pi}{2}\frac{\omega}{k}\right) \qquad \text{(where } C \text{ = a constant)}$$

and the minimum of α^2 is

$$\alpha^2 = \frac{\pi^2}{4k^2} \frac{\int_{-\frac{\pi}{2}}^{\frac{\pi}{2}} \sin^2\phi \, d\phi}{\int_{-\frac{\pi}{2}}^{\frac{\pi}{2}} \cos^2\phi \, d\phi} = \frac{\pi^2}{4k^2}$$

Thus beam-width parameter α^2 and aperture-width parameter $k = \frac{\pi d}{\lambda}$ satisfy the inequality

$$\alpha k \geq \frac{\pi}{2}$$

with equality if and only if a cosine illumination function is used. Such an illumination function is in common use in antennas.

In summary, we may observe from the above results that

(1) to have a narrow beam antenna pattern it is necessary but not sufficient to have a broad illumination,

(2) phase $\Phi(\omega)$ of the illumination function, other than a constant or a linear phase (which shifts the antenna pattern without changing its shape) increases the beam width of the antenna pattern, and there is no upper bound for this increase.

2. REVIEW OF SPECTRAL THEORY

We now want to review time-frequency aspects of signals. Many significant achievements in engineering theory may be traced to Fourier analysis which has been found to be extremely well-suited to the precise mathematical statement of many natural phenomena. An important characteristic of the Fourier method is that it gives completely equivalent statements in either the time domain or the frequency domain.

There are three main models for the Fourier approach that can be set up, namely

(1) the Fourier series approach, with the attendant assumption that the time function is a periodic function of continuous time, with the result that the spectrum is made up of lines at discrete frequencies that are integer multiples of the fundamental frequency (equal to the reciprocal of the period).

(2) the Fourier integral approach, with the attendant assumption that the time function is an aperiodic integrable function of continuous time, with the result that the spectrum is also an aperiodic integrable function of continuous frequency.

(3) the z-transform approach, with the attendant assumption that the time function is a function of equally-spaced discrete time, with the result that the spectrum is a periodic function of frequency. Hence the spectrum is a Fourier series with the time function as its Fourier coefficients.

For the purposes of this section, we shall use model (2): the Fourier integral approach. The classical

definition of the Fourier transform is as follows: Given a time-function $f(t)$, then its Fourier transform $F(\omega)$ is the frequency-function given by

$$F(\omega) = \int_{-\infty}^{\infty} f(t)\, e^{-i\omega t}\, dt$$

where

t = time (say, in seconds)
ω = radian frequency (say, in radians per second).

It is necessary to state various further remarks about $f(t)$ and $F(\omega)$, but we will assume that the reader is already familiar with them. Making use of the Euler identity

$$e^{-i\omega t} = \cos \omega t - i \sin \omega t$$

we see that the Fourier transform $F(\omega)$ is

$$F(\omega) = \int_{-\infty}^{\infty} f(t) \cos \omega t\, dt - i \int_{-\infty}^{\infty} f(t) \sin \omega t\, dt$$

= (cosine transform) - i (sine transform).

Much of our discussion will be concerned with the cosine transform for a parallel discussion would apply to the sine transform.

It is often the case that only a finite portion of the time function is available. As a result an error would result in the computation of the cosine transform because of the use of a finite instead of an infinite interval of integration. This error, called the truncation error, can be of major consequence, and so we will discuss various approaches to this problem in this section. The effect of the truncation error on transforms is to superimpose a relatively large amplitude ripple upon the correct transform; this ripple is often called the Gibbs phenomenon. Hence we will look for various suitable modified computational techniques that lessen this spurious ripple. More specifically we will look for some suitable function $w(t)$ that we shall call the <u>time gate</u> associated with the approximating method.

Denoting the Fourier transform operator by F and the approximation operator by F_A, we have

$$F[w(t)f(t)] = F_A[f(t)] = F_A(\omega)$$

for the approximate transform $F_A(\omega)$.

The Fourier transform of the time gate $w(t)$ is called the frequency window $W(\omega)$; that is,

$$W(\omega) = F[w(t)].$$

Because

$$F(\omega) = F[f(t)]$$

we can find the approximation $F_A[f(t)]$ in terms of $W(\omega)$ and $F(\omega)$. We use the familiar rule that the transform of a product is equal to the convolution of the transforms of each factor in the product. Thus

$$F_A[f(t)] = F[w(t)f(t)] = W(\omega) * F(\omega)$$

where $*$ denotes convolution, that is

$$W(\omega) * F(\omega) \equiv \frac{1}{2\pi} \int_{-\infty}^{\infty} W(\omega - \omega_1) F(\omega_1) \, d\omega_1$$

Thus we see that the approximation $F_A[f(t)]$ is obtained from the correct transform $F(\omega)$ by convolution of the correct transform with the frequency window. Let us now look at the process of convolution in order to see how the approximation differs from the correct transform. We see that $W(\omega - \omega_1)$ is the same as $W(\omega_1)$ reversed in frequency direction and shifted by the amount ω. Taking the product

$$W(\omega - \omega_1) F(\omega_1)$$

and integrating over ω_1 gives the value of the approximate transform at the frequency ω. Hence it may be said that we "look through" the frequency window (reversed and centered at ω) at the correct transform in order to obtain the approximate transform.

The frequency window is independent of the time function being transformed; instead, it is characteristic of the approximation method used and gives a complete measure of the difference between the correct transform and the approximate transform for any time function. Ideally we would

like the frequency window to be the Dirac delta function for then the approximate transform would be identical with the correct transform. Practically we will seek a frequency window $W(\omega)$ that approximates the delta function; then the convolution process for a given frequency averages the correct transform over a narrow band of frequencies around this frequency, with almost no contribution from frequencies far away from this given frequency.

Let us now turn our attention to some gates and their windows. We have the following table:

TIME GATE	FREQUENCY WINDOW
Box car of length $2T$: $w(t) = \begin{cases} 1 & \text{for } \lvert t\rvert \leq T \\ 0 & \text{for } \lvert t\rvert > T \end{cases}$ $\equiv g_0(t)$	Dirichlet window: $W(\omega) = 2T \frac{\sin \omega T}{\omega T}$ $\equiv Q_0(\omega)$
Triangle of length $2T$: $w(t) = \begin{cases} 1 - \frac{\lvert t\rvert}{T} & \text{for } \lvert t\rvert \leq T \\ 0 & \text{for } \lvert t\rvert > T \end{cases}$	Fejer window: $W(\omega) = T \left(\frac{\sin \frac{\omega T}{2}}{\frac{\omega T}{2}} \right)^2$
Delta function at t_0: $\delta(t - t_0)$	$e^{-i\omega t_0}$

TIME GATE	FREQUENCY WINDOW
Cosine wave: $\cos \omega_0 t$	$\frac{1}{2}[\delta(\omega+\omega_0)+\delta(\omega-\omega_0)]$
Von Hann gate: $w(t) = \begin{cases} \frac{1}{2}(1+\cos\frac{\pi t}{T}) & \text{for } \lvert t\rvert \le T \\ 0 & \text{for } \lvert t\rvert > T \end{cases}$	Von Hann window: $W(\omega) = \frac{1}{4}Q_0(\omega+\frac{\pi}{T})+\frac{1}{2}Q_0(\omega)+\frac{1}{4}Q_0(\omega-\frac{\pi}{T})$ where $Q_0(\omega) = 2T\frac{\sin\omega T}{\omega T}$
Richard Hamming gate: $w(t) = \begin{cases} 0.54+0.46\cos\frac{\pi t}{T} & \text{for } \lvert t\rvert \le T \\ 0 & \text{for } \lvert t\rvert \ge T \end{cases}$	Richard Hamming window: $W(\omega) = 0.23Q_0(\omega+\frac{\pi}{T})+0.54Q_0(\omega)$ $+0.23Q_0(\omega-\frac{\pi}{T})$
$w(t) = e^{i\omega_0 t}g_0(t)$	$W(\omega) = \delta(\omega-\omega_0) * Q_0(\omega) = Q_0(\omega-\omega_0)$
$w(t) = \cos\omega_0 t\, g_{60}(t)$	$W(\omega) = \frac{1}{2}[Q_0(\omega+\omega_0)+Q_0(\omega-\omega_0)]$
Ross gate: $w_k(t) = \begin{cases} (1-\frac{t^2}{T^2})^{k-1} & \text{for } \lvert t\rvert \le T \\ 0 & \text{for } \lvert t\rvert > T \end{cases}$	$W_k(\omega)$

The following result is known from the theory of the Fourier transform:

> If a time function has $n-1$ continuous derivatives and at most a step discontinuity in its n^{th} derivative, then its Fourier transform will have an envelope of order $1/\omega^{n+1}$.

Let us use this result to compare the above time gates. The box car has step discontinuities in its 0^{th} derivative; hence its window has an envelope of the order of $\frac{1}{\omega}$, as seen by the actual expression for the window. The triangle has step discontinuities in its 1^{st} derivative; hence its window has an envelope of the order $\frac{1}{\omega^2}$, as seen by the actual expression. The Von Hann gate has step discontinuities in its second derivative; hence its window has an $\frac{1}{\omega^3}$ envelope. The Ross gate $W_k(t)$ has step discontinuities in its $k-1$ derivative; hence its window has an $\frac{1}{\omega^k}$ envelope.

It is interesting to consider the characteristics of the family of Ross gates. The first few members are plotted in the following diagram:

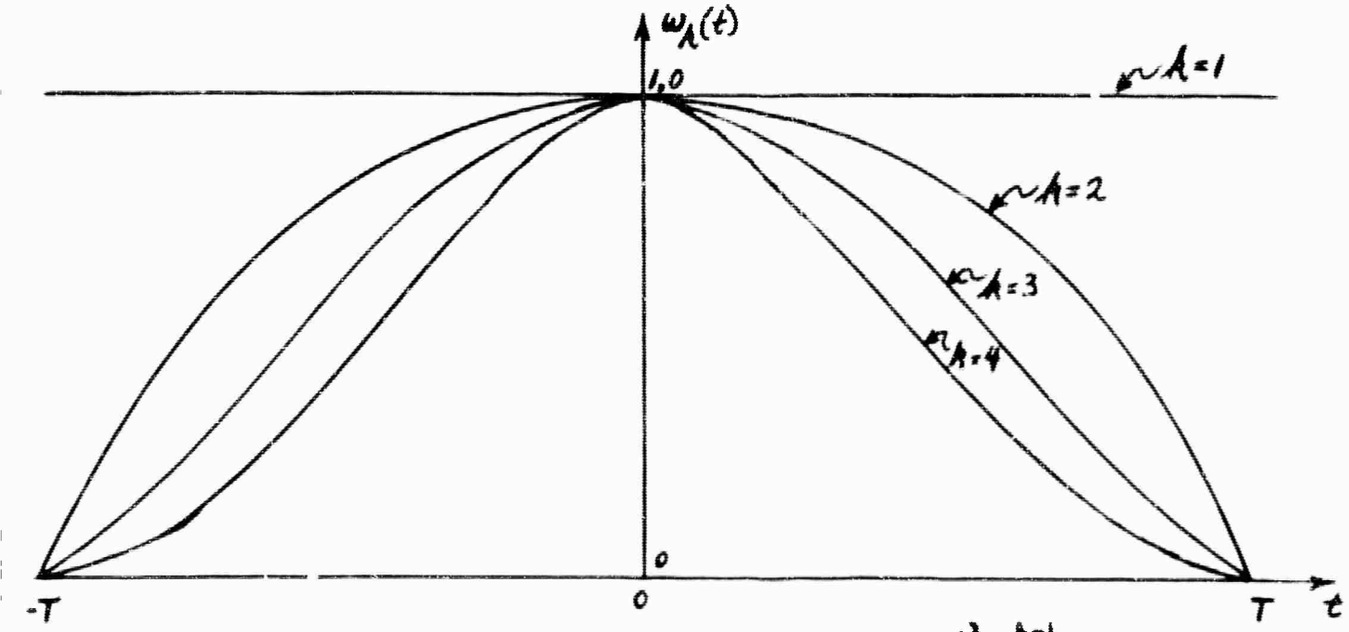

Figure 2. The family of time gates $W_k(t)=\left(1-\frac{t^2}{T^2}\right)^{k-1}$

We see that higher values of λ means less and less contribution from values whose abcissa is close to $t = \pm T$.

Let us now find an interpretation for this family. Let us consider the case where the function to be transformed is

$$f(t) = \cos \omega t$$

for some arbitrary frequency ω . This choice has the advantage that we know that the normalized correct transform of this function is unity for ω and zero for all other frequencies. The problem is to find out what is the effect of calculating the approximate transform given by

$$\frac{2}{T}\int_0^T f(t) \cos \omega_1 t \, dt$$

instead of the correct transform given by

$$\lim_{T\to\infty} \frac{2}{T}\int_0^T f(t) \cos \omega_1 t \, dt ,$$

and how the result varies for T and ω_1 . The frequency ω_1 may be called the <u>scanning frequency</u>.

For the case when $\omega_1 = \omega$, the approximate transform is

$$\frac{2}{T}\int_0^T \cos^2 \omega t \, dt = 1 + \frac{\sin 2\omega T}{2\omega T}$$

and for the case when $\omega_1 \neq \omega$, the approximate transform is

$$\frac{2}{T}\int_0^T \cos\omega t \cos\omega_1 t \, dt = \frac{\sin(\omega-\omega_1)T}{(\omega-\omega_1)T} + \frac{\sin(\omega+\omega_1)T}{(\omega+\omega_1)T}$$

The result $1+\frac{\sin 2\omega T}{2\omega T}$ for the case $\omega_1=\omega$ is plotted in the figure.

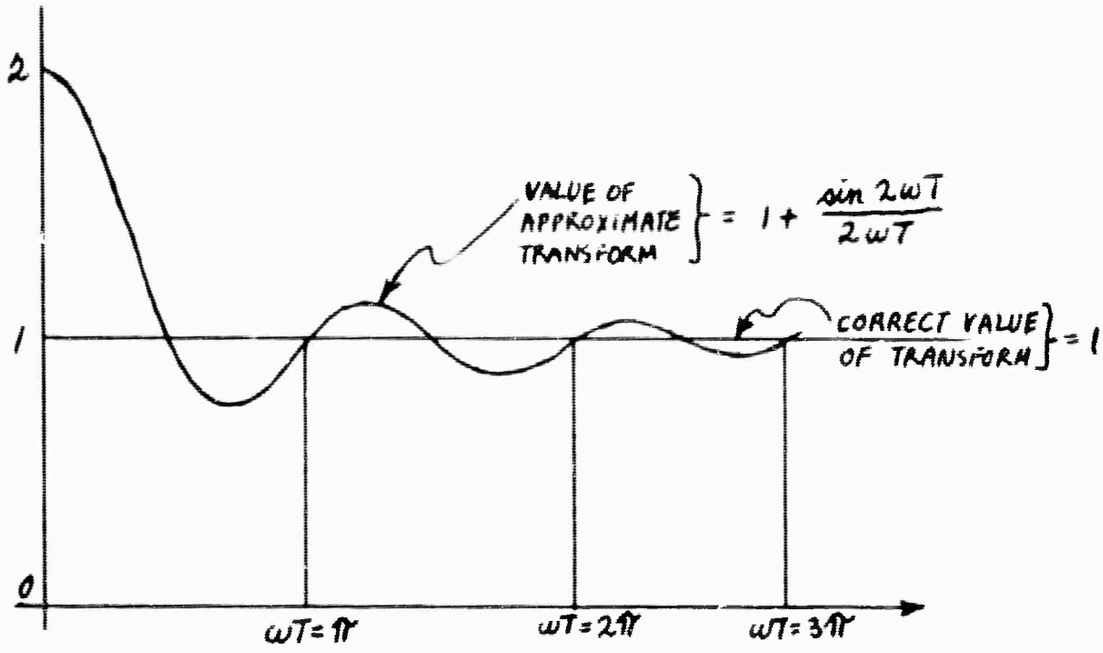

Figure 3. Dependence of the approximate transform on truncation length T.

From the figure we see that the approximation oscillates about the correct answer, 1, and gets closer and closer to this correct answer as T is increased. The problem now is to find a way to utilize this oscillating approximation so as to find a more refined approximation. It appears that a linear weighting of the oscillating estimate shown in the figure would be a good choice, and in fact corresponds to Fejer summation of the original integral.

We thus have

$$\int_0^T \frac{2t}{T^2}\left(1+\frac{\sin 2\omega t}{2\omega t}\right)dt = 2\left(\frac{1}{2}+\frac{1-\cos 2\omega T}{4\omega^2 T^2}\right)$$

$$= 1+\frac{\sin^2 \omega T}{(\omega T)^2}$$

This function is plotted in the figure:

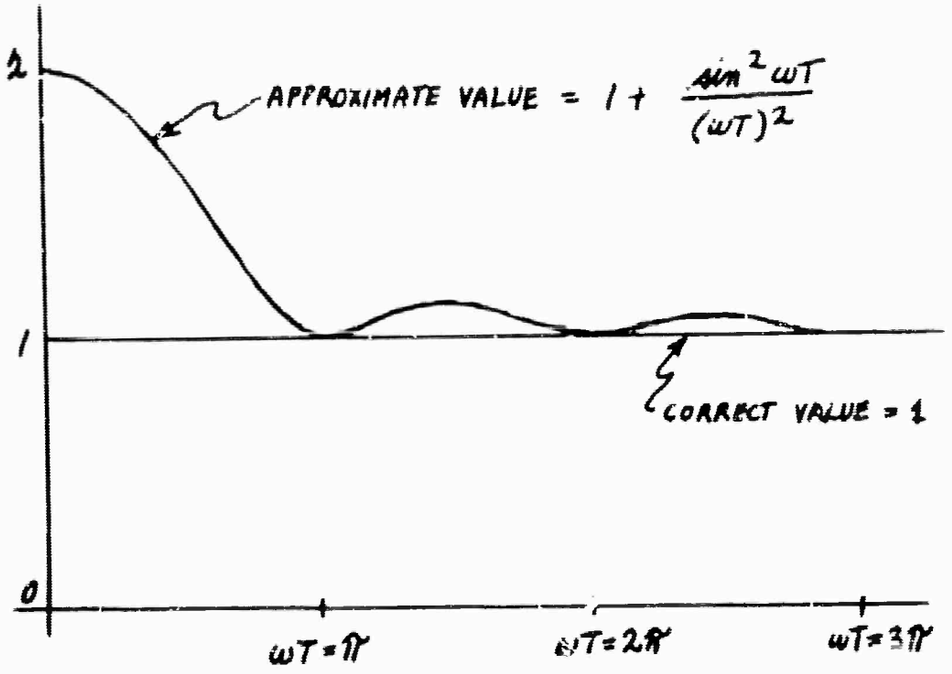

Figure 4. Dependence of the second approximate transform on truncation length T.

For most T values, this function is closer to the correct value, 1, than the previous approximation, and thus the weighting has helped matters to some extent. The envelope of this approximation is $\frac{1}{(\omega T)^2}$. Nevertheless, this choice of weighting has introduced the problem that the approximation no longer oscillates about the correct value

For the third approximation let us choose the weighting function $3t^2/T^3$, thereby obtaining:

$$\int_0^T \frac{3t^2}{T^3}\left(1+\frac{\sin 2\omega t}{2\omega t}\right)dt = 1+\frac{3}{(2\omega T)^2}\left(\frac{\sin 2\omega T}{2\omega T}-\cos 2\omega T\right)$$

This function not only has the $\left(\frac{1}{\omega T}\right)^2$ envelope, but also the approximation still oscillates about the correct value, which means that the process can be continued.

For the scanning frequency $\omega_1 \neq \omega$, this approximation is

$$\frac{3}{T^2}\left[\frac{1}{(\omega-\omega_1)^2}\left(\frac{\sin(\omega-\omega_1)T}{(\omega-\omega_1)T}-\cos(\omega-\omega_1)T\right)\right.$$

$$\left.+\frac{1}{(\omega+\omega_1)^2}\left(\frac{\sin(\omega+\omega_1)T}{(\omega+\omega_1)T}-\cos(\omega+\omega_1)T\right)\right]$$

which has the same order envelope around the correct value 0.

We are now in a position to derive the Ross class of time gates. The first stage gives the (unnormalized) approximation

$$\int_0^{t_1} f(t)\cos\omega t\, dt$$

The second stage gives

$$\int_0^{t_2} t_1 dt_1 \int_0^{t_1} f(t)\cos\omega t\, dt$$

Interchanging the order of integration, this expression becomes

$$\int_0^{t_2} f(t)\cos\omega t\,dt \int_t^{t_2} t_1 dt_1 = \int_0^{t_1} \left(\frac{t_2^2 - t^2}{2}\right) f(t)\cos\omega t\,dt$$

so the second stage corresponds to the weighting function or time gate

$$\frac{t_2^2 - t^2}{2}$$

Similarly the time gates for higher stages can be found.

It is instructive to look upon the Ross time gates $W_k(t)$ as a means of countering the effects of truncation by smoothing the approximation at the price of losing a certain amount of frequency information. When $f(t)$ is multiplied by $W_k(t)$, the effect is to make the values of $f(t)$ for large $|t|$ not as important in the approximation as those for small t. This leads to smoothing since each successive value contributes less and less to the accumulated integral. Nevertheless, if we take a time gate $W_k(t)$ for a too large value of k, then we essentially reject a very large portion of the given finite record of $f(t)$; and the resulting approximation achieved by using a more moderate value of k. Thus, if we try to achieve too much smoothing, we may sacrifice significant frequency information; it is necessary to strike a balance between these two conflicting goals. Excellent empirical and theoretical treatment of this problem is given in the original work of Ross (1954).

3. MULTICHANNEL SPIKING AND SHAPING FILTERS

First we wish to consider properties of polynomials orthogonal on the unit circle (Geronimus, 1960). The polynomials $\phi_n(z)$ are defined to be orthonormal with respect to the spectral density $\Phi(f)$ on the unit circle $|z|=1$; that is,

$$\int_{-0.5}^{0.5} \phi_n(e^{-2\pi i f})\,\overline{\phi_m(e^{-2\pi i f})}\,\Phi(f)\,df = \begin{cases} 0 & n \neq m \\ 1 & n = m \end{cases}$$

where $\phi_n(z) = \alpha_n z^n + \beta_n z^{n-1} + \cdots + w_n$ with $\alpha_n > 0$.

Also let us define

$$\phi_n^*(z) = z^n \overline{\phi_n}\left(\frac{1}{z}\right) \qquad \text{so} \qquad \phi_n^*(0) = \alpha_n$$

Let us put

$$\frac{\phi_n(z) - \alpha_n z^n}{z^{n-1}} = \beta_n + \gamma_n \frac{1}{z} + \delta_n \frac{1}{z^2} + \cdots + w_n \frac{1}{z^{n-1}}$$

$$= \mu_0^{(n)} \overline{\phi}\left(\frac{1}{z}\right) + \mu_1^{(n)} \overline{\phi}_1\left(\frac{1}{z}\right) + \cdots + \mu_{n-1}^{(n)} \overline{\phi}_{n-1}\left(\frac{1}{z}\right),$$

and then multiply each side by $\phi(z)$ for $k = 0, 1, 2, \cdots, n-1$, set $z = e^{-2\pi i f}$, and integrate.

We obtain

$$\mu_k^{(n)} = \int_{-0.5}^{0.5} \phi_n(e^{-2\pi i f}) \frac{\phi_k(e^{-2\pi i f})}{e^{-2\pi i (n-1) f}} \Phi(f)\, df$$

$$- \alpha_n \int_{-0.5}^{0.5} e^{-2\pi i f} \phi_k(e^{-2\pi i f}) \Phi(f)\, df$$

Since $\phi_k(e^{-2\pi i f}) / e^{-2\pi i (n-1) f}$ is a polynomial in $e^{+2\pi i j f}$ where $j < n$ it follows that the first integral is zero, and by introducing the notation

$$\lambda_k = \int_{-\frac{1}{2}}^{\frac{1}{2}} z\, \phi_k(z) \Phi(f)\, df \quad \text{with} \quad z = e^{-2\pi i f} \quad \text{for} \quad k = 0, 1, 2, \cdots$$

we obtain $\mu_k^{(n)} = -\alpha_n \lambda_k$

and hence

$$\frac{\phi_n(z)}{\alpha_n} = z^n - z^{n-1} \sum_{k=0}^{n-1} \lambda_k \bar{\phi}_k\left(\frac{1}{z}\right)$$

$$\frac{\phi_{n+1}(z)}{\alpha_{n+1}} = z^{n+1} - z^n \sum_{k=0}^{n} \lambda_n \bar{\phi}_k\left(\frac{1}{z}\right)$$

so

$$\frac{\phi_{n+1}(z)}{\alpha_{k+1}} - \frac{z\,\phi_n(z)}{\alpha_n} = -\lambda_n \phi_n^*(z)$$

By setting $Z = 0$ we find λ_n ; that is,

$$\frac{\Phi_{n+1}(0)}{\alpha_{n+1}} = -\lambda_n \Phi_n^*(0) = -\lambda_n \alpha_n$$

so

$$\lambda_n = -\frac{\Phi_{n+1}(0)}{\alpha_n \alpha_{n+1}}$$

Thus

$$\frac{\Phi_{n+1}(Z)}{\alpha_{n+1}} - \frac{Z\Phi_n(Z)}{\alpha_n} = \frac{\Phi_{n+1}(0)}{\alpha_{n+1}} \frac{\Phi_n^*(Z)}{\alpha_n}$$

so the following recursion relation holds;

$$\boxed{\frac{\Phi_{n+1}(Z)}{\alpha_{n+1}} = \frac{Z\Phi_n(Z)}{\alpha_n} + \frac{\Phi_{n+1}(0)}{\alpha_{n+1}} \frac{\Phi_n^*(Z)}{\alpha_n}}$$

In this relation, let us replace Z by $\frac{1}{Z}$, thereby obtaining

$$\frac{\Phi_{n+1}(\frac{1}{Z})}{\alpha_{n+1}} = \frac{(\frac{1}{Z})\Phi_n(\frac{1}{Z})}{\alpha_n} + \frac{\Phi_{n+1}(0)}{\alpha_{n+1}} \frac{\Phi_n^*(\frac{1}{Z})}{\alpha_n}$$

and multiplying by Z^{n+1} and taking complex conjugates we obtain

$$\frac{Z^{n+1}\overline{\Phi}_{n+1}(\frac{1}{Z})}{\alpha_{n+1}} = \frac{Z^n \overline{\Phi}_n(\frac{1}{Z})}{\alpha_n} + \frac{\overline{\Phi_{n+1}(0)}}{\alpha_{n+1}} \frac{Z Z^n \overline{\Phi}_n^*(\frac{1}{Z})}{\alpha_n}$$

which is the recursion relation

$$\boxed{\frac{\Phi_{n+1}^*(z)}{\alpha_{n+1}} = \frac{\Phi_n^*(z)}{\alpha_n} + \frac{\overline{\Phi_{n+1}(0)}}{\alpha_{n+1}} \frac{z\,\Phi_n(z)}{\alpha_n}}$$

Let us introduce the polynomials

$$\Psi_n(z) = \frac{\Phi_n(z)}{\alpha_n}, \quad \Psi_n^*(z) = z^n \overline{\Psi_n}\left(\frac{1}{z}\right),$$

and define the parameters a_n by the formula

$$a_n = -\overline{\Psi_{n+1}(0)} = -\frac{\overline{\Phi_{n+1}(0)}}{\alpha_{n+1}} \qquad \text{for } n = 0, 1, 2, \cdots$$

Then the recursion relations become

$$\boxed{\begin{aligned} \Psi_{n+1}(z) &= z\,\Psi_n(z) - \bar{a}_n \Psi_n^*(z) \\ \Psi_{n+1}^*(z) &= \Psi_n^*(z) - a_n z\,\Psi_n(z) \end{aligned}}$$

Let us now find the connection between the parameter a_n and the autocorrelation

$$r_k = \int_{-\frac{1}{2}}^{\frac{1}{2}} e^{2\pi i k f}\, \Phi(f)\, df = \bar{r}_{-k}.$$

The Toeplitz determinant is defined to be

$$\Delta_k = |r_{i-j}|_0^k = \begin{vmatrix} r_0 & r_{-1} & \cdots & r_{-k} \\ r_1 & r_0 & & r_{-k+1} \\ \cdots & & & \\ r_k & r_{k-1} & \cdots & r_0 \end{vmatrix}, \quad k = 0, 1, 2, \cdots; \ \Delta_{-1} = 1;$$

and it is seen that the polynomials can be written

$$\psi_n(z) = \frac{1}{\Delta_{n-1}} \begin{vmatrix} r_0 & r_{-1} & r_{-2} & \cdots & r_{-n} \\ r_1 & r_0 & r_{-1} & & r_{-n+1} \\ & & & & \\ r_{n-1} & r_{n-2} & r_{n-3} & & r_{-1} \\ 1 & z & z^2 & & z^n \end{vmatrix} = z^n + \cdots - \bar{a}_{n-1}.$$

Let us introduce the notation

$$(\phi(z), \xi(z)) \equiv \int_{-\frac{1}{2}}^{\frac{1}{2}} \phi(e^{-2\pi i f}) \overline{\xi(e^{-2\pi i f})}\, \Phi(f)\, df$$

where $\phi(z)$ and $\xi(z)$ are arbitrary polynomials in z. Using this notation we see that

$$(\psi_n, \psi_n) = (\psi_n(z), z^n) = \frac{1}{\Delta_{n-1}} \begin{vmatrix} r_0 & r_{-1} & r_{-n} \\ r_1 & r_0 & r_{-n+1} \\ & & \\ r_{n-1} & r_{n-2} & r_{-1} \\ (1, z^n) & (z, z^n) & (z^n, z^n) \end{vmatrix}$$

$$= \frac{1}{\Delta_{n-1}} \begin{vmatrix} r_0 & r_{-1} & r_{-n} \\ r_1 & r_0 & r_{-n+1} \\ & & \\ r_{n-1} & r_{n-2} & r_{-1} \\ r_n & r_{n-1} & r_0 \end{vmatrix} = \frac{\Delta_n}{\Delta_{n-1}}$$

$$= \frac{1}{\alpha_n^2} \qquad \text{since} \quad (z^k, z^n) = r_{n-k}.$$

From the relations

$$\psi_{n+1} = z\psi_n - \bar{a}_n \psi_n^*$$

$$\psi_{n+1}^* = \psi_n^* - a_n z \psi_n$$

it is possible to find a recursion involving only ψ_n^* as follows. Solving for ψ_n we find

$$\psi_n = \frac{\psi_n^* - \psi_{n+1}^*}{a_n^2}$$

and hence

$$\frac{\psi_{n+1}^* - \psi_{n+2}^*}{a_{n+1} z} = \frac{\psi_n^* - \psi_{n+1}^*}{a_n} - \bar{a}_n \psi_n^*$$

which gives

$$a_n \psi_{n+2}^* = (a_n + a_{n+1} z)\psi_{n+1}^* - a_{n+1} z (1 - |a_n|^2)\psi_n^*.$$

Similarly, we find that

$$\bar{a}_n \psi_{n+2} = (\bar{a}_n z + \bar{a}_{n+1})\psi_{n+1} - \bar{a}_{n+1} z (1 - |a_n|^2)\psi_n.$$

From this last expression we obtain

$$\bar{a}_n(\psi_{n+2}, z^{n+1}) = \bar{a}_n(z\psi_{n+1}, z^{n+1}) + \bar{a}_{n+1}(\psi_{n+1}, z^{n+1}) - \bar{a}_{n+1}(1 - |a_n|^2)(z\psi_n, z^{n+1})$$

which is

$$\frac{1}{d_{n+1}^2} - (1 - |a_n|^2)\frac{1}{d_n^2} = 0$$

since

$$\frac{1}{d_{n+1}^2} = (\psi_{n+1}, \psi_{n+1}) = (\psi_{n+1}, z^{n+1}).$$

so

$$\frac{\alpha_n^2}{\alpha_{n+1}^2} = 1 - |a_n|^2$$

Thus

$$\frac{1}{\alpha_n^2} = \frac{\Delta_n}{\Delta_{n-1}} = \frac{1}{\alpha_0^2} \prod_{k=0}^{n-1} (1 - |a_k|^2) \quad \text{where } \frac{1}{\alpha_0^2} = r_0$$

and

$$\frac{1}{\alpha_n^2} = \frac{1}{\alpha_0^2} - \frac{|a_0|^2}{\alpha_0^2} - \frac{|a_1|^2}{\alpha_1^2} - \cdots - \frac{|a_{n-1}|^2}{\alpha_{n-1}^2}$$

This last step follows by induction since

$$\frac{1}{\alpha_{n+1}^2} = \left(\frac{1}{\alpha_0^2} - \frac{|a_0|^2}{\alpha_0^2} - \frac{|a_1|^2}{\alpha_1^2} - \cdots - \frac{|a_{n-1}|^2}{\alpha_{n-1}^2} \right)(1 - |a_n|^2)$$

$$= \left(\frac{1}{\alpha_0^2} - \frac{|a_0|^2}{\alpha_0^2} - \frac{|a_1|^2}{\alpha_1^2} - \cdots - \frac{|a_{n-1}|^2}{\alpha_{n-1}^2} \right) - \frac{|a_n|^2}{\alpha_n^2}.$$

In summary we have

(1) $\phi_n = d_n z^n + \cdots + w_n$

(2) $(\phi_n, \phi_m) = \delta_{nm}$ = Kronecker delta function

(3) $\psi_n \equiv \frac{\phi_n}{d_n}$ so $(\psi_n, \psi_m) = \frac{1}{d_n^2}\delta_{nm}$

(4) $a_n \equiv -\overline{\psi_{n+1}(0)}$

(5) $\bar{a}_n \psi_{n+2} = (\bar{a}_n z + \bar{a}_{n+1})\psi_{n+1} - \bar{a}_{n+1} z (1-|a_n|^2)\psi_n$

(6) $(z_n, z_m) = r_{m-n}$

(7) $(\psi_n, \psi_n) = (\psi_n, z^n) = \frac{1}{d_n^2} = \frac{\Delta_n}{\Delta_{n-1}}$

$$= \frac{1}{d_0^2}(1-|a_0|^2)(1-|a_1|^2)\cdots(1-|a_{n-1}|^2)$$

$$= \frac{1}{d_0^2} - \frac{|a_0|^2}{d_0^2} - \frac{|a_1|^2}{d_1^2} - \cdots - \frac{|a_{n-1}|^2}{d_{n-1}^2}$$

where

$$\Delta_k = \det \begin{pmatrix} r_0 & r_{-1} & \cdots & r_{-k} \\ r_1 & r_0 & \cdots & r_{-k+1} \\ \cdots & & & \\ r_k & r_{k-1} & \cdots & r_0 \end{pmatrix} \quad \text{for } k = 0, 1, 2, \cdots;$$

$$\Delta_{-1} = 1, \qquad \frac{1}{d_0^2} = r_0.$$

Now let us treat the multichannel case following the methods given in the monograph Studies in Optimum Filtering of Single and Multiple Stochastic Processes. We now use matrix notation. We have the forward polynomial

$$a_n(z) = a_{no} + a_{n1} z + \cdots + a_{nn} z^n \qquad (a_{no} = I)$$

and the backward polynomial

$$b_n(\tfrac{1}{z}) = b_{nn}(\tfrac{1}{z})^n + \cdots + b_{n1}(\tfrac{1}{z}) + b_{no} \qquad (b_{no} = I)$$

where

$$[a_{no}, \cdots, a_{nn}, 0] \begin{bmatrix} r_0 & \cdots & r_{n+1} \\ \cdots & & \\ r_{-n-1} & \cdots & r_0 \end{bmatrix} = [\alpha_n, 0, \cdots, 0, \alpha_n']$$

with $\alpha_n' = a_{no} r_{n+1} + \cdots + a_{nn} r_1$

and

$$[0, b_{nn}, \cdots, b_{no}] \begin{bmatrix} r_0 & \cdots & r_{n+1} \\ \cdots & & \\ r_{-n-1} & \cdots & r_0 \end{bmatrix} = [\beta_n', 0, 0, \cdots, 0, \beta_n]$$

with $\beta_n' = b_{nn} r_1 + \cdots + b_{no} r_{-n-1}$.

(Note, this is a new use of the symbol α, corresponding to the usage in the above monograph).

Thus

$$[a_{n0}, a_{n1}+k_{an}b_{nn}, \cdots, k_{an}b_{n0}]\begin{bmatrix} r_0 & \cdots & r_{n+1} \\ \cdots & & \\ r_{-n-1} & \cdots & r_0 \end{bmatrix}$$

$$= [\alpha_n + k_{an}\beta'_n, 0, \cdots, 0, \alpha'_n + k_{an}\beta_n]$$

and

$$[k_{bn}a_{n0}, b_{nn}+k_{bn}a_{n1}, \cdots, b_{n0}]\begin{bmatrix} r_0 & \cdots & r_{n+1} \\ \cdots & & \\ r_{-n-1} & \cdots & r_0 \end{bmatrix}$$

$$= [\beta'_n + k_{bn}\alpha_n, 0, \cdots, 0, \beta_n + k_{bn}\alpha'_n]$$

where k_{an} and k_{bn} are chosen so that

$$\alpha'_n + k_{an}\beta_n = 0 \,, \qquad \beta'_n + k_{bn}\alpha_n = 0$$

The new filters are

$$[a_{n+1,0}, a_{n+1,1}, \cdots, a_{n+1,n+1}] = [a_{n0}, \cdots a_{nn}, 0] + k_{an}[0, b_{nn}, \cdots b_{n0}]$$

and

$$[b_{n+1,n+1}, \cdots, b_{n+1,1}, b_{n+1,0}] = [0, b_{nn}, \cdots, b_{n0}] + k_{bn}[a_{n0}, \cdots a_{an}, 0]$$

where

$$k_{an} = -\alpha'_n\beta_n^{-1} = a_{n+1,n+1} \,, \quad k_{bn} = -\beta'_n\alpha_n^{-1} = b_{n+1,n+1}.$$

Thus the polynomials satisfy the recursion formulae:

$$\boxed{\begin{aligned} a_{n+1}(z) &= a_n(z) + k_{an}z^{n+1}b_n\left(\tfrac{1}{z}\right) \\ b_{n+1}\left(\tfrac{1}{z}\right) &= b_n\left(\tfrac{1}{z}\right) + k_{bn}\left(\tfrac{1}{z}\right)^{n+1}a_n(z) \end{aligned}}$$

The new α_{n+1} and β_{n+1} are given by

$$\begin{aligned}\alpha_{n+1} &= \alpha_n + k_{an}\beta_n' \\ &= \alpha_0 + k_{a0}\beta_0' + k_{a1}\beta_1' + \cdots + k_{a,n-1}\beta_{n-1}' + k_{an}\beta_n' \\ &= \alpha_n - k_{an}k_{bn}\alpha_n \\ &= \alpha_0 - k_{a0}k_{b0}\alpha_0 - k_{a1}k_{b1}\alpha - \cdots - k_{an}k_{bn}\alpha_n\end{aligned}$$

and

$$\begin{aligned}\beta_{n+1} &= \beta_n + k_{bn}\alpha_n' \\ &= \beta_n - k_{bn}k_{an}\beta_n \\ &= \beta_0 - k_{b0}k_{a0}\beta_0 - k_{b1}k_{a1}\beta_1 - \cdots - k_{bn}k_{an}\beta_n\end{aligned}$$

These are the analogues of the formulae found in the single channel case, just given.

The general filter polynomial is

$$f_n(z) = f_{n0} + f_{n1}z + f_{n2}z^2 + \cdots + f_{nn}z^n$$

where

$$[f_{n0}, f_{n1}, \cdots, f_{nn}, 0]\begin{bmatrix} r_0 & \cdots & r_{n+1} \\ & \cdots & \\ r_{-n-1} & \cdots & r_0 \end{bmatrix} = [g_0, \cdots, g_n, \gamma_{n+1}]$$

with $\gamma_{n+1} = f_{n0}r_{n+1} + \cdots + f_{nn}r_1$.

Thus

$$\left[f_{n0} + k_{fn} b_{n+1,n+1}, \cdots, f_{nn} + k_{fn} b_{n+1,1}, k_{fn} b_{n+1,0}\right] \begin{bmatrix} r_0 & \cdots & r_{n+1} \\ & \cdots & \\ r_{n+1} & \cdots & r_0 \end{bmatrix}$$

$$= \left[g_0, \cdots, g_n, \gamma_{n+1} + k_{fn} \beta_{n+1}\right].$$

Thus the new general filter is obtained by setting

$$\gamma_{n+1} + k_{fn} \beta_{n+1} = g_{n+1}$$

so

$$\left[f_{n+1,0}, \cdots, f_{n+1,n}, f_{n+1,n+1}\right]$$
$$= \left[f_{n,0}, \cdots, f_{n,n}, 0\right] + k_{fn}\left[b_{n+1,n+1}, \cdots, b_{n+1,1}, b_{n+1,0}\right]$$

Thus the general filter polynomial satisfies the recursion

$$\boxed{f_{n+1}(z) = f_n(z) + k_{fn} z^{n+1} b_{n+1}\left(\tfrac{1}{z}\right)}$$

In particular:

$$f_1(z) = f_0(z) + k_{f0} z\, b_1\left(\tfrac{1}{z}\right)$$
$$f_2(z) = f_1(z) + k_{f1} z^2 b_2\left(\tfrac{1}{z}\right)$$
$$f_3(z) = f_2(z) + k_{f2} z^3 b_3\left(\tfrac{1}{z}\right)$$

so

$$f_3(z) = f_0(z) + k_{f0} z\, b_1\left(\tfrac{1}{z}\right) + k_{f1} z^2 b_2\left(\tfrac{1}{z}\right) + k_{f2} z^3 b_3\left(\tfrac{1}{z}\right)$$

and hence:

$$f_n(z) = f_0(z) + k_{f0} z\, b_1\left(\tfrac{1}{z}\right) + k_{f1} z^2 b_2\left(\tfrac{1}{z}\right) + \cdots + k_{f,n-1} z^n b_n\left(\tfrac{1}{z}\right).$$

Likewise:

$$a_n(z) = a_0(z) + k_{a0} z\, b_0\left(\frac{1}{z}\right) + k_{a1} z^2\, b_1\left(\frac{1}{z}\right) + \cdots + k_{a,n-1} z^n\, b_{n-1}\left(\frac{1}{z}\right)$$

$$b_n(z) = b_0\left(\frac{1}{z}\right) + k_{b0}\left(\frac{1}{z}\right) a_0(z) + k_{b1}\left(\frac{1}{z}\right)^2 a_1(z) + \cdots + k_{b,n-1}\left(\frac{1}{z}\right)^n a_{n-1}(z)$$

where $b_0(z) = b_0$, $a_0(z) = a_0$, $b_0\left(\frac{1}{z}\right) = b_0$

are constant matrices.

4. SEISMIC ARRAYS

A seismic disturbance except in special cases does not reach each detector in an array at the same instant, and so there is a time difference between corresponding phase points of the disturbance recorded at different spatial locations. This time difference can be expressed in units of time per unit of distance, and thus is the reciprocal of the phase velocity.

Let us consider the following model. The signals from distant events arrive at the array with horizontal velocities ranging from infinity (that is, the case of vertical incidence) to some finite minimum value. The noise, on the other hand, is assumed to have horizontal velocities smaller than the minimum set for the signals, and such lower velocities are indeed to be expected of surface wave noise. Thus in this model seismic signals and seismic noise have different velocity distributions, and therefore improvement in signal-to-noise ratio can be expected through the use of a device that discriminates against noise velocities. Such a device is called a velocity filter, and for the model that we have assumed it should be a high-pass velocity filter, that is, one that passes high velocities and stops low velocities.

Let us consider a plane wave front. Because a two-dimensional group of detectors is equivalent to a one-dimensional group in a plane perpendicular to the wave front, we shall limit the present discussion to one dimensional arrays. A plane wave of a fixed temporal frequency f_t and spatial frequency f_x may be written

$$\sin(2\pi f_t t + 2\pi f_x x + \theta)$$

where θ is an arbitrary constant representing a phase displacement. The quantity $1/f_t$ is the period and the quantity $1/f_x$ is the wave length. The phase velocity along the array is given by

$$v = \frac{f_t}{f_x}$$

We may suppose that the above quantities are expressed in units as follows:

f_t = temporal frequency, in cycles per second (c/s)

$1/f_t$ = period, in seconds per cycle (s/c)

f_x = spatial frequency, in cycles per kilometer (c/km)

$1/f_x$ = wavelength, in kilometers per cycle (km/c)

v = velocity, in kilometers per second (km/s)

$= f_t/f_x = (1/f_x)/(1/f_t)$ = (wavelength) / (period)

The output of a so-called uniformly distributed array of $n+1$ elements over a distance Δ is equal to the sum of the outputs from each detector. See figure 5.

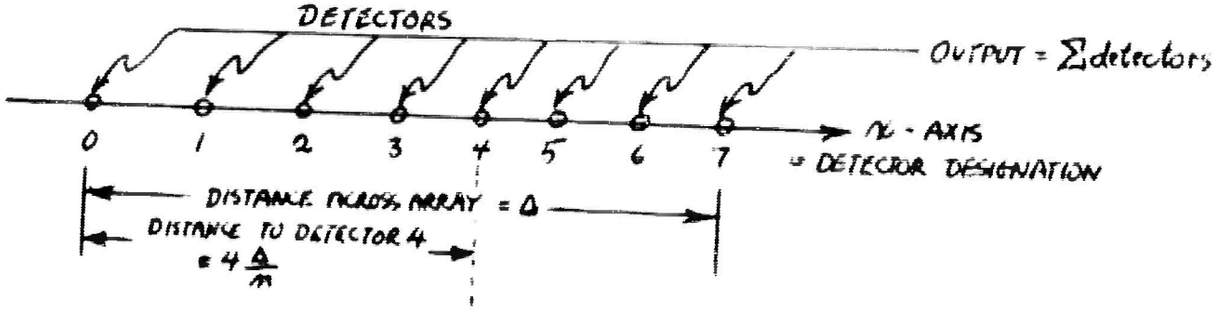

Figure 5. Uniformly distributed array ($n = 7$).

Hence the output to the above sinusoidal input would be (normalized by the factor $1/n+1$)

$$\frac{1}{n+1}\sum_{k=0}^{n}\sin\left(2\pi f_t t + 2\pi f_x \frac{k\Delta}{n} + \beta\right)$$

which is equal to

$$\frac{\sin\left(\frac{n+1}{n}\pi f_x \Delta\right)}{(n+1)\sin\left(\frac{\pi f_x \Delta}{n}\right)}\sin\left(2\pi f_t t + \pi f_x \Delta + \beta\right)$$

Thus the transfer function, namely the ratio of output to input, is at the center of the array

$$A_n = \frac{\sin\left(\frac{n+1}{n}\pi f_x \Delta\right)}{(n+1)\sin\left(\frac{\pi f_x \Delta}{n}\right)}$$

If we let $n \to \infty$, then A_n becomes the transfer ratio of a continuous detector whose length is Δ ; we have

$$A_\infty = \frac{\sin \pi f_x \Delta}{\pi f_x \Delta}$$

Let us introduce the dimensionless spatial frequency variable $\nu = f_x \Delta$. Then we have

$$A_n = \frac{\sin\left(\frac{n+1}{n}\pi\nu\right)}{(n+1)\sin\left(\frac{\pi\nu}{n}\right)} \quad , \quad A_\infty = \frac{\sin \pi\nu}{\pi\nu} .$$

The figure shows graphs of $A_2(\nu)$, $A_3(\nu)$, and $A_\infty(\nu)$.

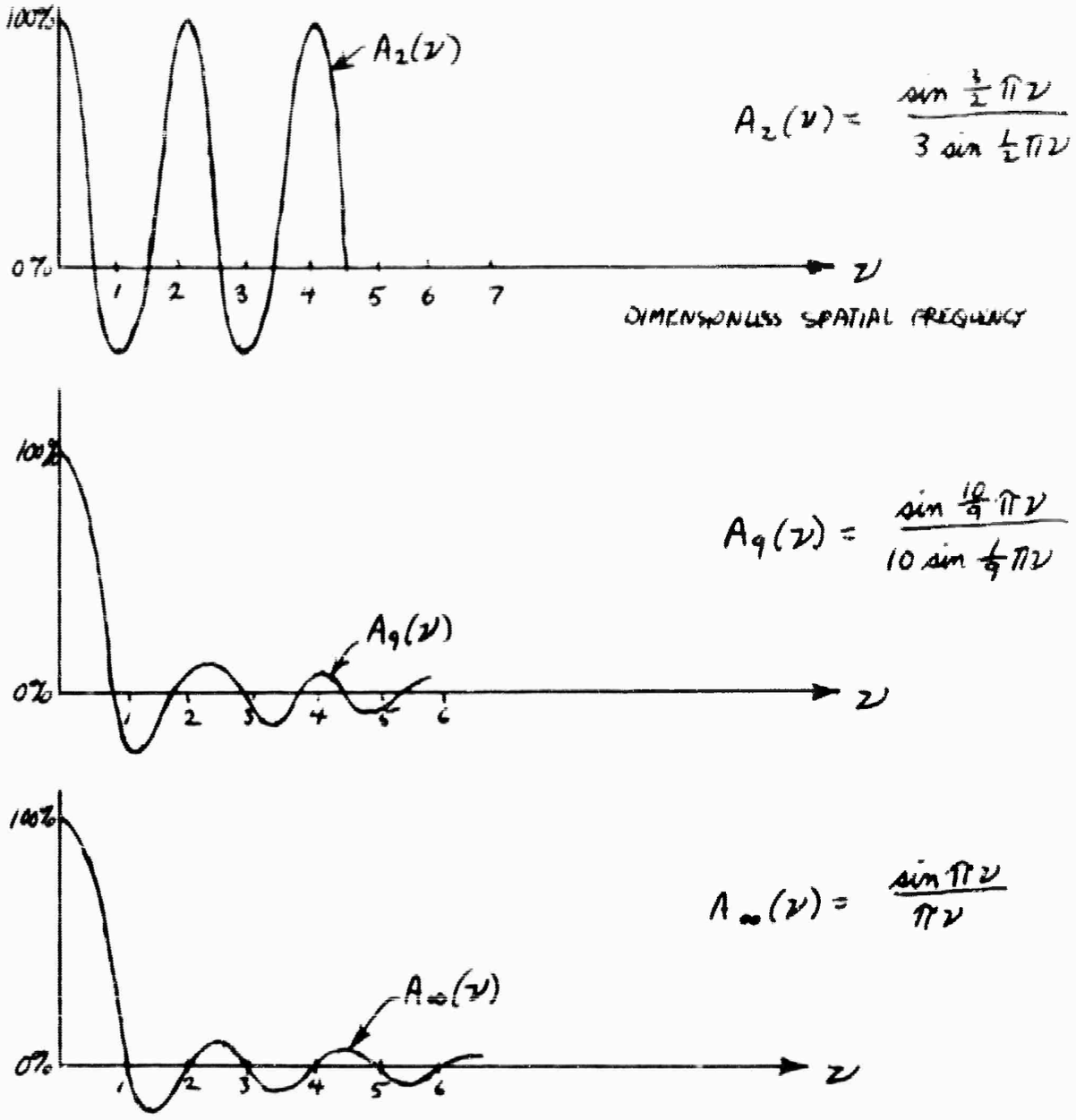

Figure 6. Graphs of spatial frequency transfer functions

Provided the noise corresponding to values of $\nu > 6$ is negligible, it is seen that increasing the number, $n+1$, of seismometers in the array beyond 10 can yield no appreciable improvement in velocity discrimination under the scheme of uniform spacing and uniform weighting of the seismometers in the array.

For example, let us suppose that the ambient noise is spatially organized and is propagating with an apparent horizontal velocity of 4 km/s. Suppose that one component of the noise has a temporal frequency f_t = 1 c/s; and that the other component of the noise has a temporal frequency f_t = 0.5 c/s. Suppose that one component of the signal is made up of mantle P-waves travelling at a velocity of 8 km/s and with a temporal frequency f_t = 1 c/s; that the other component of the signal has the same velocity (8 km/s) and a temporal frequency f_t = 2 c/s. Thus we have the table (where wavelength λ = the reciprocal of the spatial frequency).

TEMPORAL FREQUENCY f_t	SIGNAL Velocity v = 8 km/s	NOISE Velocity v = 4 km/s
$f_t = 0.5$ c/s		$\lambda = 8$ km, $\nu = \frac{1}{2}$
$f_t = 1.0$ c/s	$\lambda = 8$ km, $\nu = \frac{1}{2}$	$\lambda = 4$ km, $\nu = 1$
$f_t = 2.0$ c/s	$\lambda = 4$ km, $\nu = 1$	

TABLE: Wavelength λ and dimensionless spatial frequency ν vs. velocity v and temporal frequency f_t, where $\lambda = \frac{v}{f_t}$, and $\nu = f_x \Delta = \frac{\Delta}{\lambda}$ with $\Delta = 4$ km.

We recall that the transfer function $A_\infty(\nu)$ has the shape:

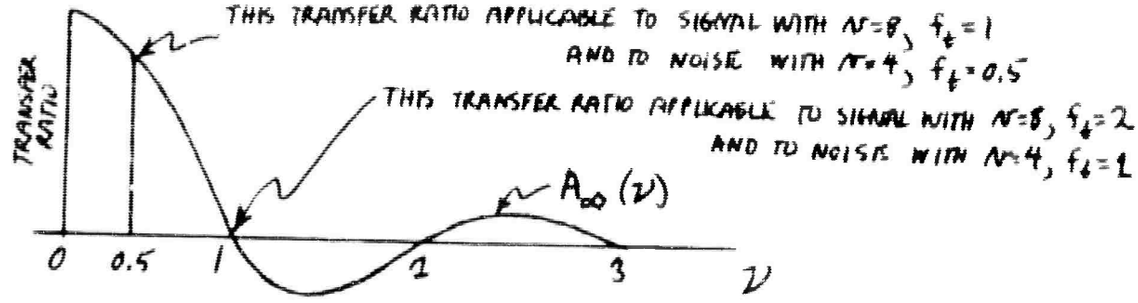

Figure 7. Transfer function of $A_\infty(\nu)$.

We see that the maximum wavelength that can be completely filtered out is equal to the array of length Δ, so the minimum length of the array is dictated by the maximum wave length which is desirable to have filtered out. Thus we have the filtering action of the array given by the table:

SIGNAL $N = 8$	NOISE $N = 4$
	f_t = 0.5 c/s (PASSED)
f_t = 1 c/s (PASSED)	f_t = 1 c/s (STOPPED)
f_t = 2 c/s (STOPPED)	

TABLE: PASS and STOP bands of array, with spread Δ = 4 km.

Thus for 8 km/s P-waves this array with uniform summation provides maximum effectiveness only over a small fraction of an octave around the temporal frequency f_t = 1 c/s.

Now let us consider an array with equally spaced detectors but where each detector is weighted by an arbitrary factor before summation. We suppose that we have $2n+1$ detectors of arbitrary sensitivity at locations $x = 0, \pm\frac{\Delta}{n}, \pm\frac{2\Delta}{n}, \cdots, \pm\Delta$ with sensitivities $1, a_1, a_2, \cdots, a_3$ . . If the input is

$$\cos(2\pi f_t t + 2\pi f_x x + \beta)$$

then the output is

$$\cos(2\pi f_t t + \beta)\left[1 + 2\sum_{j=1}^{n} a_j \cos\left(2\pi f_x \frac{j\Delta}{n}\right)\right]$$

so the transfer ratio is

$$A_n = 1 + 2\sum_{j=1}^{n} a_j \cos\left(2\pi f_x j \frac{\Delta}{n}\right)$$

We see that A_n is a periodic function of f_x . When $f_x = C$ we have

$$A_n = 1 + 2\sum_{j=1}^{n} a_j \qquad (f_x \neq 0);$$

when $f_x = \frac{n}{\Delta}$ we have

$$A_n = 1 + 2\sum_{j=1}^{n} a_j \qquad \left(f_x = \frac{n}{\Delta}\right).$$

Thus the period of A_n corresponds to $f_x = \frac{n}{\Delta}$, which is a wavelength $\lambda = \frac{\Delta}{n}$, namely the detector spacing of the array. In other words, the array cannot distinguish between the following two situations:

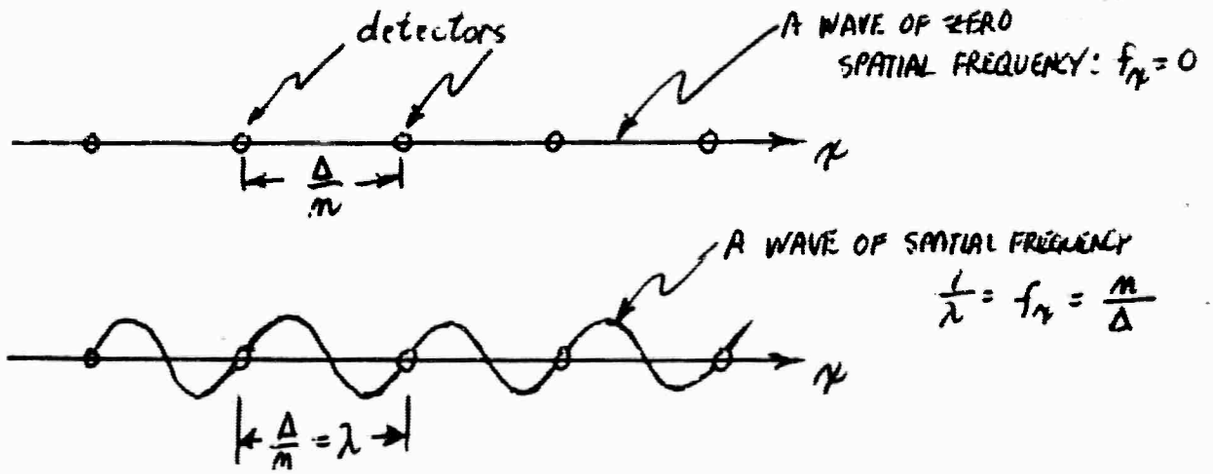

Figure 8. Illustration of aliasing.

This phenomenon is well-known, and is called aliasing. Thus it is desirable to choose the detector spacing such that the 100% response peaks that occur after $f_x = 0$ do not correspond to wavelengths that are associated with substantial energy.

Suppose the following values of a_j are chosen (Savit, Brustad, and Sider, 1958):

$a_0 = 1.000$
$a_1 = 0.987$
$a_2 = 0.947$
$a_3 = 0.888$
$a_4 = 0.809$
$a_5 = 0.704$
$a_6 = 0.592$
$a_7 = 0.473$
$a_8 = 0.348$
$a_9 = 0.224$
$a_{10} = 0.105$

The transfer ratio in terms of dimensionless spatial frequency

$$\nu = f x \Delta$$

is

$$A_n(\nu) = 1 + 2 \sum_{j=1}^{n} a_j \cos\left(2\pi j \frac{\nu}{n}\right).$$

Graphs of a_j and $A_n(\nu)$ are shown in the figure

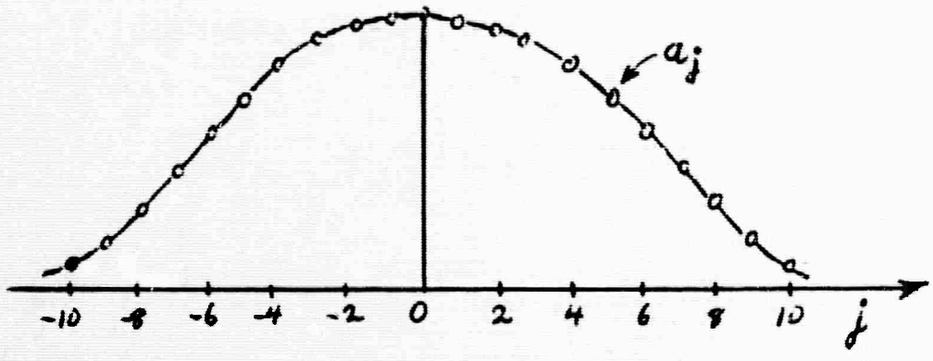

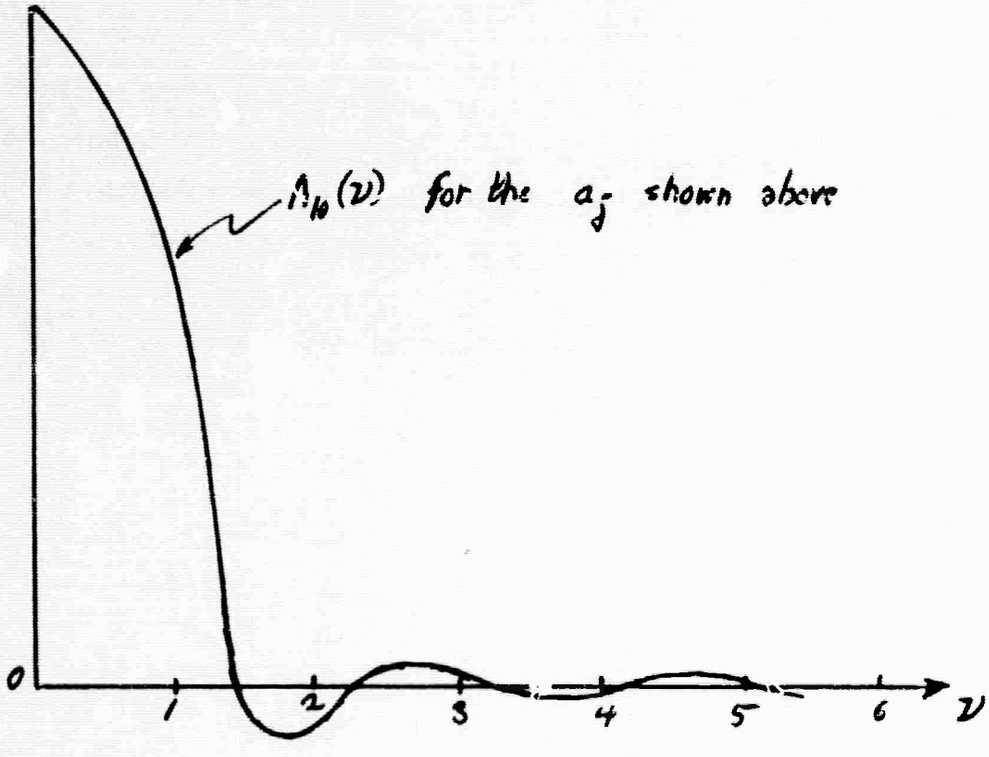

Figure 9. Weighting function a_j and corresponding transfer function $A_{10}(\nu)$.

5. VELOCITY FILTERING

The concept of filtering seismic signals based on their apparent velocities is treated by Texas Instruments Staff (1961), Embree et al (1963) and Fail and Graw (1963). Such velocity filtering for the nuclear surveillance problem is implemented by the use of large arrays of seismometers. Velocity filtering, then, is a multichannel filtering process. The process uses a number of input channels from the seismometers to produce each output, but differs from conventional mixing and filtering techniques in that each input at a different delay is filtered through a different appropriately designed filter response before being summed to form the output.

In order to design such a multichannel filter, a working model of signal and noise must be formulated in the temporal and spatial frequency domain. In addition, criteria for judging the performance of the arrays must be established. The theoretical requirements for optimum processing have to be developed with the quantitative evaluation of the performance.

The primary objective of large array systems is to provide a better picture of the seismic signals when they are masked by ambient noise. A large array should make it possible to detect and identify seismic events that are obscured by ambient noise when only a single sensor is used.

The complexity of the seismic waves that arrive at a detection station is well-known. For either an earthquake or an explosion source, the following sequence of seismic

waves is produced:

(1) P-waves, or longitudinal body waves. They have a propagation velocity of about 6 to 8 km/s, depending on the medium.

(2) S-waves, or transverse body waves. They travel at 0.6 times the velocity of P-waves.

(3) Love waves, or horizontal transverse surface waves. They travel along the earth's surface at a velocity of 4 to 4.5 km/s.

(4) Rayleigh waves, or vertical surface waves that perform a retrograde elliptical motion with its plane lying along the axis of propagation.

The P and S waves are subject to reflections and refractions, and the surface waves undergo dispersion. The result is a complex sequence of oscillations whose nature is governed by the characteristics of the transmission paths and very little by the source itself. Since the only part of the wave train that arrives undisturbed by later modes is the P wave (the first arrival), it is the most important signal currently used for location and identification of the source. Secondary objectives are the extraction of S-waves and surface waves in the presence of noise.

The noise obscuring the desired signals may be categorized as follows:

(a) Ambient coherent microseismic noise, propagating primarily as Rayleigh waves, with an apparent horizontal velocity of 2.5 to 3.5 km/s. The isotropic assumption means that the noise is equally likely to come from any azimuth.

(b) Local coherent noise from sources such as factories, lakes, railroads, highways, propagating primarily as Rayleigh waves, but with a particular azimuth of propagation.

(c) Incoherent noise from sources or scatterers within the array area, including locally generated wind noise.

(d) Incoherent instrument noise.

The P-wave signal may be characterized as follows:

(a) Coherent
(b) Equally likely to come from any azimuth
(c) Apparent horizontal propagation velocity of 8 to 15 km/s.

The signal and noise can be shown in the three dimensional temporal and spatial frequency domain, whose axis are f_t, f_x, f_y . For example, a propagating sinusoidal plane wave is a point in the f_t, f_x, f_y domain, even as a sine wave $\sin 2\pi f_t t$ is a point in the f_t domain. The signal and coherent noise in the working model are continued in the conical boundaries shown in the figure:

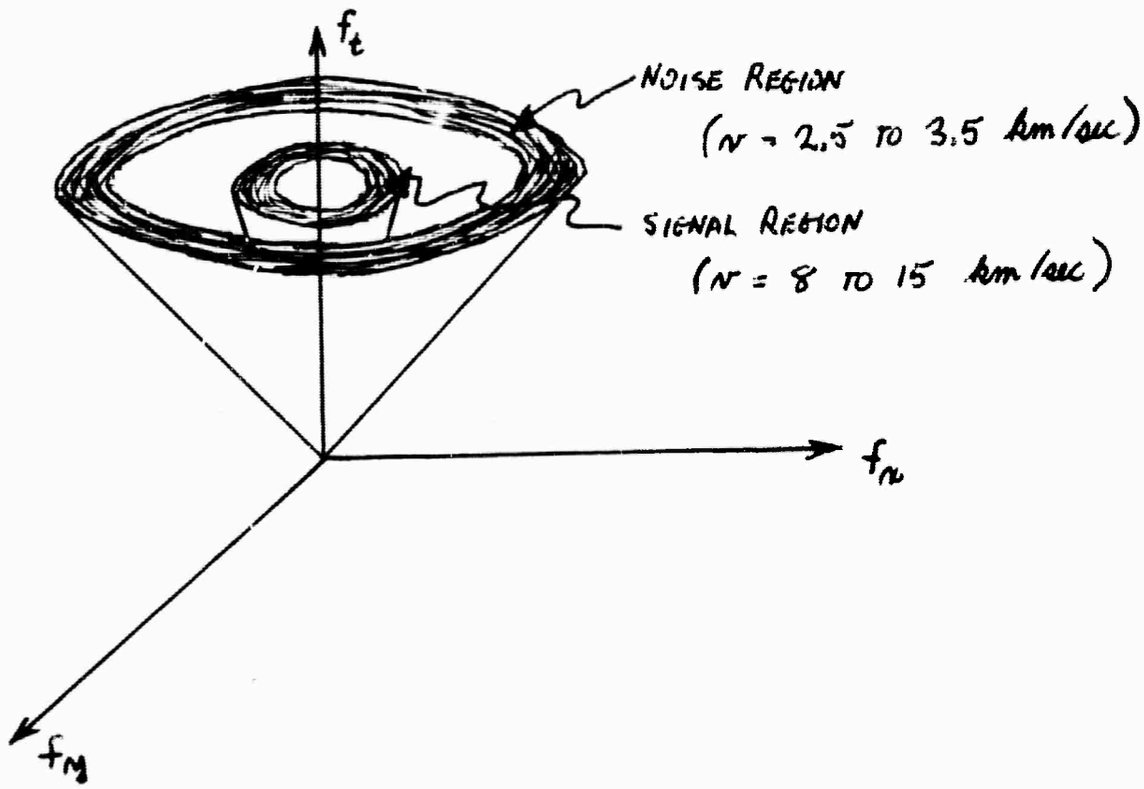

Figure 10. Signal and noise in three dimensional frequency domain.

Assuming that the signal propagates with a speed of from 8 to 15 km/s, and is equally-likely to arrive from any azimuth, the signal power lies within the conical boundaries shown in the figure. The total power at any frequency f_t may be obtained by integrating over all f_x, f_y for that f_t, and it is assumed to be the curve shown in the figure:

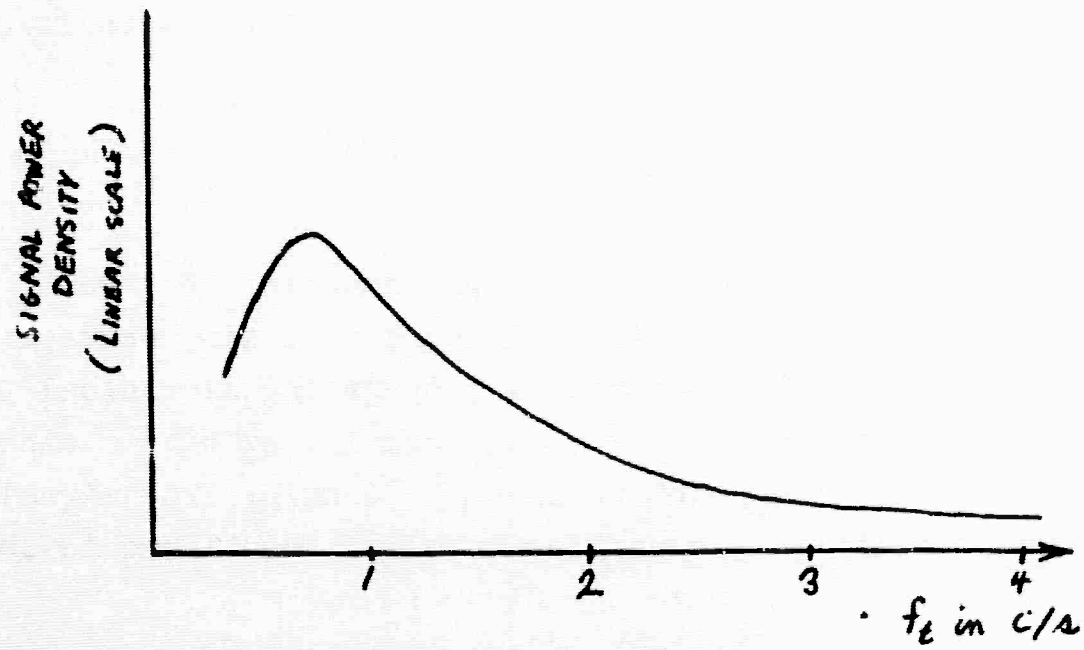

Figure 11. Signal power density spectrum

The noise power lies between the two cones corresponding to velocities of 2.5 to 3.5 km/s, and by integrating over f_x and f_y we assume the power density has the form in the f_t domain as shown in the figure:

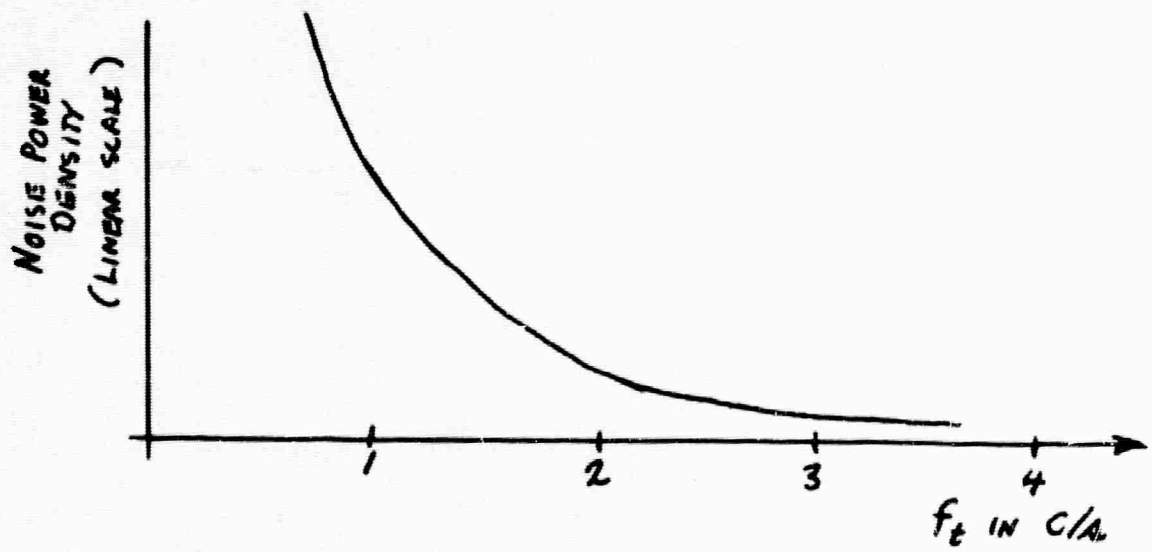

Figure 12. Coherent noise power density spectrum

Incoherent noise at a particular frequency f_t is uniformly distributed over the entire f_x, f_y plane.

For the isotropic model, a vertical cut in the f_t, f_x, f_y space is independent of azimuth, as shown in the figure:

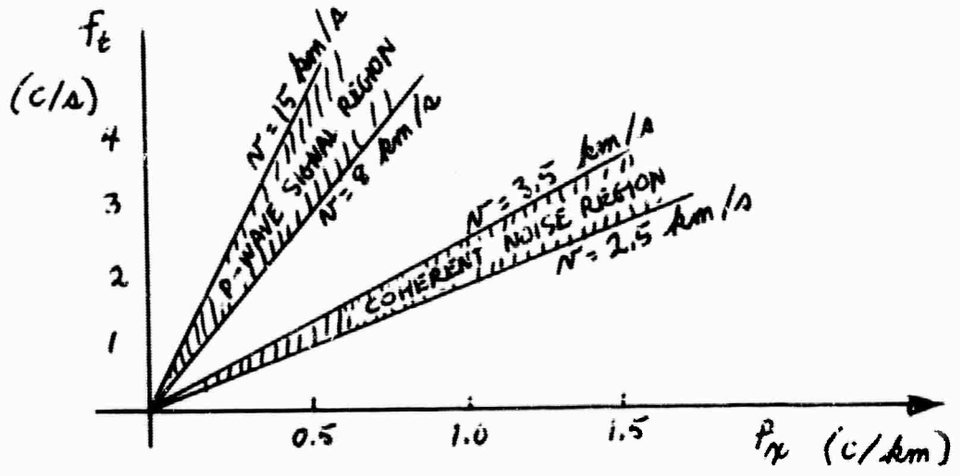

Figure 13. A vertical slice of Figure 10

For a directional signal model, the three dimensional space must be retained.

This working model of seismic signal and noise has the following important features:

(a) The signal and coherent noise are completely separable in f_t, f_x, f_y space. This separability is unique to the seismic case; in radar, sonar, and radio astronomy the signal and noise propagation velocities are identical and so separation can be achieved only on a directional basis. The maximum, improvement in such cases is $\sqrt{N}$ (in amplitude) in signal-to-isotropic noise ratio by an N element array; because the signal and coherent noise are completely separable in the seismic case, greater gains are possible, and the achievable gain is dependent on the temporal and spatial distribution of the noise.

(b) The signal and incoherent noise are not completely separable, and hence this noise cannot be as effectively reduced by an array. Achievable array gains are thus critically dependent on the power ratio of incoherent noise to coherent noise.

Let us now consider the actual implementation of the velocity filter. We want the filter to pass waves in the velocity range from $-V$ to $+V$, so the desired response in temporal and spatial frequency is

$$A(f_t, f_x) = \begin{cases} 0 & \text{for } f_x < -\dfrac{|f_t|}{V} \\ 1 & \text{for } -\dfrac{|f_t|}{V} < f_x < \dfrac{|f_t|}{V} \\ 0 & \text{for } \dfrac{|f_t|}{V} < f_x \end{cases}$$

This transfer function is depicted in the diagram:

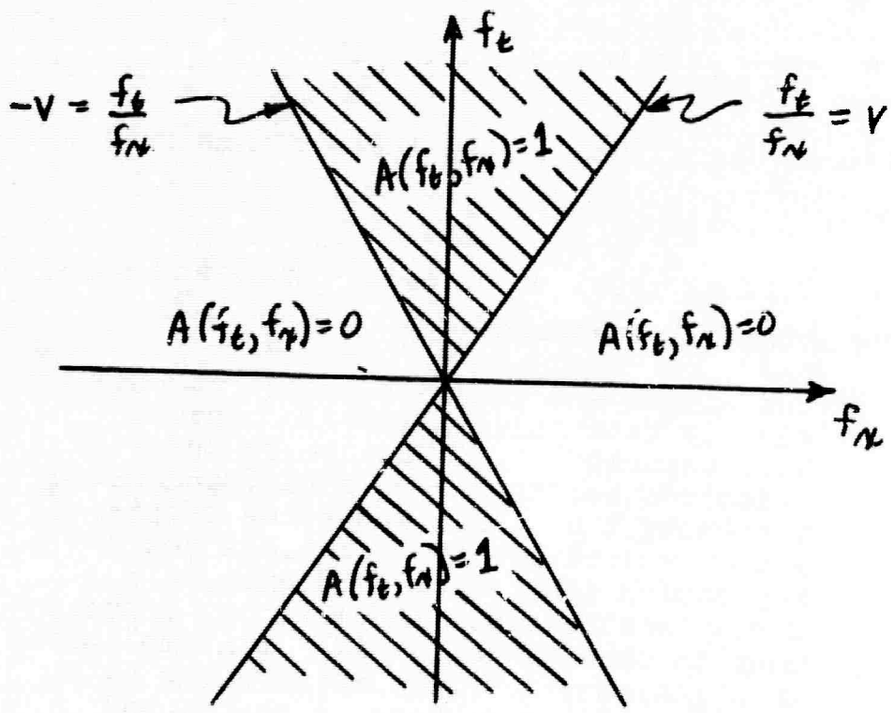

Figure 14. Desired spectral response function of velocity filter

At a given frequency f_t the spatial impulse response is

$$a(f_t, x) = \int_{f_x=-\frac{|f_t|}{V}}^{f_x=\frac{|f_t|}{V}} e^{-2\pi i f_x x}\, df_x$$

$$= \int_{-\frac{|f_t|}{V}}^{\frac{|f_t|}{V}} \cos 2\pi f_x x \, df_x$$

$$= \frac{1}{2\pi x} \sin 2\pi f_x x \Big]_{-\frac{|f_t|}{V}}^{\frac{|f_t|}{V}}$$

$$= \frac{\sin 2\pi \frac{|f_t|}{V} x}{\pi x}$$

If $|f_t| = V$ then $a(f_t, x) = \frac{\sin 2\pi x}{\pi x}$, which looks like:

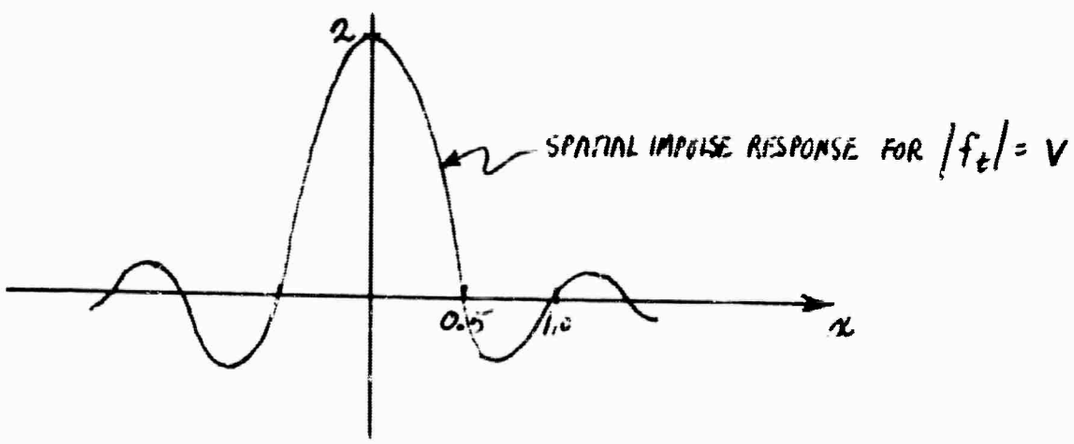

Figure 15. Spatial impulse response of desired filter for $|f_t| = V$

whereas if $|f_t| = 2V$ then $a(f_t, x) = \frac{\sin 4\pi x}{\pi x}$, which looks like:

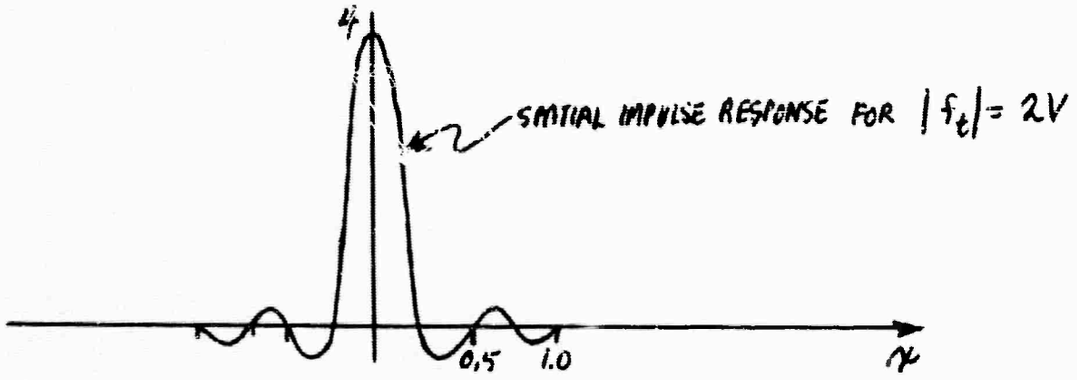

Figure 16. Spatial impulse response of desired filter for $|f_t| = 2V$.

Therefore, in terms of arrays, such a process appears at low frequencies as a very long array, which passes long wavelengths and stops short wavelengths, or in other words it acts as a narrow band low pass filter in spatial frequencies. Such a process appears at high frequencies as a very short array, which passes shorter wavelengths, or in other words, it acts as a wider band low pass filter in spatial frequencies.

The impulse response in time t and space x is given by

$$a(t,x) = \int_{-\infty}^{\infty} \int_{f_x=-\frac{|f_t|}{V}}^{f_x=\frac{|f_t|}{V}} e^{2\pi i (f_t t - f_x x)} \, df_x \, df_t$$

$$= \int_{-\infty}^{\infty} e^{2\pi i f_t t} \, a(f_t, x) \, df_t$$

$$= \int_{-\infty}^{\infty} e^{2\pi i f_t t} \, \frac{\sin(2\pi x \frac{|f_t|}{V})}{\pi x} \, df_t .$$

In the usual case, the array will be made up of equally spaced sensors with spacing Δx , as depicted by:

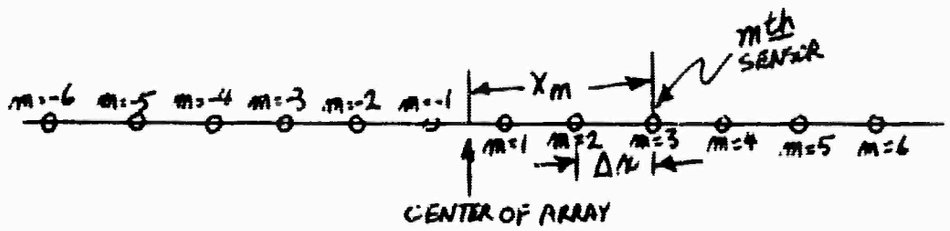

Figure 17. Sensor spacing

We suppose that there is an even number of sensors, and we let X_m denote the distance of the m^{th} sensor from the center of the array. Thus $X_1 = +\frac{1}{2}\Delta x$, $X_{-1} = -\frac{1}{2}\Delta x$, $X_2 = +\frac{3}{2}\Delta x$, etc. The process may be implemented by passing the output of each sensor through a temporal frequency filter with transfer function specified by

$$a(f_t; X_m) = \frac{\sin 2\pi \frac{|f_t|}{v} X_m}{\pi X_m}$$

and then summing the outputs of all the temporal frequency filters. The frequency spectrum $a(f_t, X_m)$ looks like

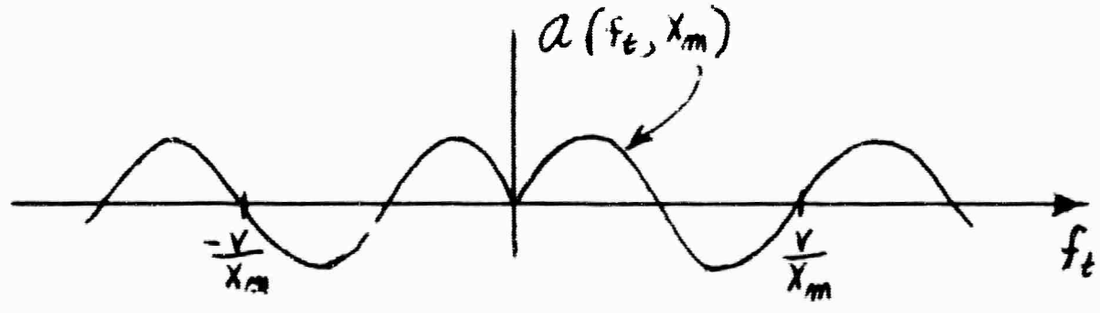

Figure 18. Frequency spectrum of $a(f_t, X_m)$

At any given temporal frequency, no array with equally spaced sensors can distinguish between zero cycles per $2\Delta x$, or any other integral number of cycles per $2\Delta x$, as shown in the figure:

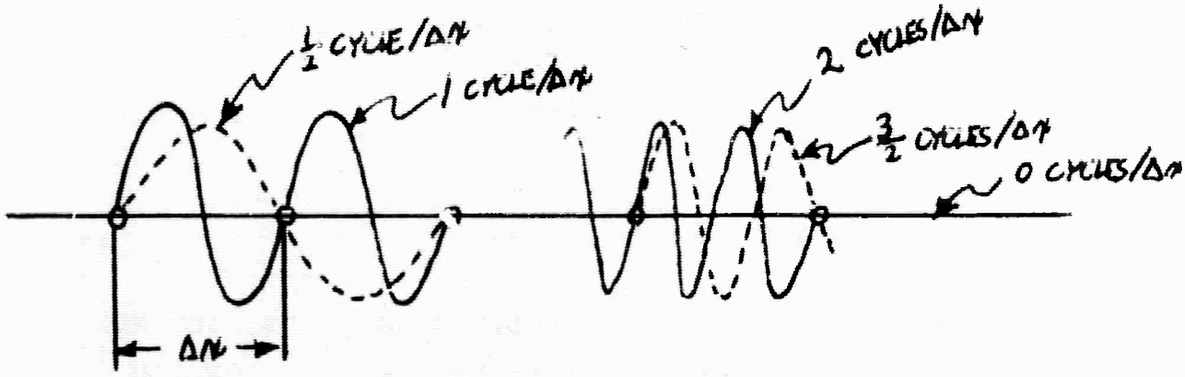

Figure 19. Spatial aliasing

Here $1/2\Delta x = f_x^N$ is the Nyquist spatial frequency (or the folding spatial frequency), and the equally spaced sensors result in a periodic response in spatial frequency, the response being repeated at the interval

$$\Delta f_x = \frac{1}{\Delta x}$$

and the desired response can be achieved only over the spatial frequency band

$$-f_x^N = -\frac{1}{2\Delta x} \leq f_x \leq \frac{1}{2\Delta x} = f_x^N.$$

At temporal frequencies above

$$|f_t^N| = f_x^N V = \frac{V}{2\Delta x}$$

the specified pass band of the velocity filter extends beyond the Nyquist spatial frequency f_x^N, so the temporal frequency range over which a useful response may be obtained is limited to temporal frequencies below f_t^N. Thus a sampling interval $\Delta t = \frac{1}{2 f_t^N}$ may be chosen, and no information is lost provided the data is limited to frequencies below f_t^N and f_x^N. If we let $T_n = n\Delta t$ be the time of the n^{th} sample point in the discrete impulse response of the time-domain filter, then we see that V satisfies

$$V = \frac{|f_t^N|}{f_x^N} = \frac{\frac{1}{2\Delta t}}{\frac{1}{2\Delta x}} = \frac{\Delta x}{\Delta t}$$

The required coefficient of the n^{th} time point of the time-domain filter for the m^{th} sensor is

$$a(T_n, X_m) = \int_{f_t=-\frac{1}{2\Delta t}}^{f_t=\frac{1}{2\Delta t}} df_t \int_{f_x=-\frac{|f_t|}{V}}^{f_x=\frac{|f_t|}{V}} df_x \, e^{2\pi i (f_t T_n - f_x X_m)}$$

$$= \int_{-\frac{1}{2\Delta t}}^{+\frac{1}{2\Delta t}} df_t \, e^{2\pi i f_t T_n} \, \frac{\sin\left(2\pi \frac{|f_t|}{V} X_m\right)}{\pi X_m}$$

$$= \frac{2}{\pi X_m} \int_0^{\frac{1}{2\Delta t}} df_t \, \cos(2\pi f_t T_n) \sin(2\pi f_t \frac{X_m}{V})$$

$$= \frac{2}{\pi X_m} \int_0^{\frac{1}{2\Delta t}} df_t \, \cos(2\pi n \Delta t f_t) \sin(2\pi \frac{X_m}{\Delta x} \Delta t f_t)$$

Now the following integration formula occurs in standard tables:

$$\int \sin ax \cos bx \, dx = -\frac{1}{2}\left[\frac{\cos(a-b)x}{a-b} + \frac{\cos(a+b)x}{a+b}\right]$$

provided $a^2 \neq b^2$. Hence

$$a(T_n, X_m) = \frac{2}{\pi X_m}(-\frac{1}{2}) \left[\frac{\cos 2\pi \Delta t (\frac{X_m}{\Delta x} - n) f_t}{2\pi \Delta t (\frac{X_m}{\Delta x} - n)} + \frac{\cos 2\pi \Delta t (\frac{X_m}{\Delta x} + n) f_t}{2\pi \Delta t (\frac{X_m}{\Delta x} + n)} \right]_{f_t = 0}^{f_t = \frac{1}{2\Delta t}}$$

$$= -\frac{1}{\pi X_m} \left[\frac{\cos \pi (\frac{X_m}{\Delta x} - n)}{2\pi \Delta t (\frac{X_m}{\Delta x} - n)} + \frac{\cos \pi (\frac{X_m}{\Delta x} + n)}{2\pi \Delta t (\frac{X_m}{\Delta x} + n)} - \frac{1}{2\pi \Delta t (\frac{X_m}{\Delta x} - n)} - \frac{1}{2\pi \Delta t (\frac{X_m}{\Delta x} + n)} \right]$$

and since $\frac{X_m}{\Delta x} = \begin{cases} m - \frac{1}{2} & \text{if } m > 0 \\ m + \frac{1}{2} & \text{if } m < 0 \end{cases}$ where m is an integer

and since n is an integer, it follows that

$$\frac{X_m}{\Delta x} \pm n$$

is equal to an integer divided by 2, so the first two terms in the expression for $a(T_n, X_m)$ above vanish. Hence

$$a(T_n, X_m) = \frac{1}{\pi X_m}\left[\frac{1}{2\pi \Delta t}\right]\left[\frac{1}{\frac{X_m}{\Delta x} - n} + \frac{1}{\frac{X_m}{\Delta x} + n}\right]$$

$$= \frac{1}{2\pi^2 X_m \Delta t}\left[\frac{(\frac{X_m}{\Delta x} + n) + (\frac{X_m}{\Delta x} - n)}{(\frac{X_m}{\Delta x} - n)(\frac{X_m}{\Delta x} + n)}\right]$$

$$= \frac{1}{\pi^2 \Delta x \Delta t} \frac{1}{(\frac{X_m}{\Delta x})^2 - n^2}$$

where

$$T_n = n\Delta t \quad , \qquad n = 0, \pm 1, \pm 2, \cdots$$

$$X_m = \begin{cases} (m - \frac{1}{2})\Delta x \ , & m = 1, 2, 3, \cdots \\ (m + \frac{1}{2})\Delta x \ , & m = -1, -2, -3, \cdots \end{cases}$$

It is seen that the linear operator $a(T_n, X_m)$ is symmetric about the origin in both space and time.

The theoretical frequency response can be recovered by

$$A(f_t, f_x) = \sum_{n=-\infty}^{\infty} \sum_{\substack{m=-\infty \\ m \neq 0}}^{\infty} a(T_n, X_m)\, e^{-2\pi i (f_t T_n - f_x X_m)}$$

In practice only a finite number of n and m values can be used, so the theoretical frequency response is only approximated. In case $n = 0, \pm 1, \pm 2, \pm 3, \cdots, \pm 10$ and $m = \pm 1, \pm 2, \cdots, \pm 6$ then the actual response is as depicted in the figure:

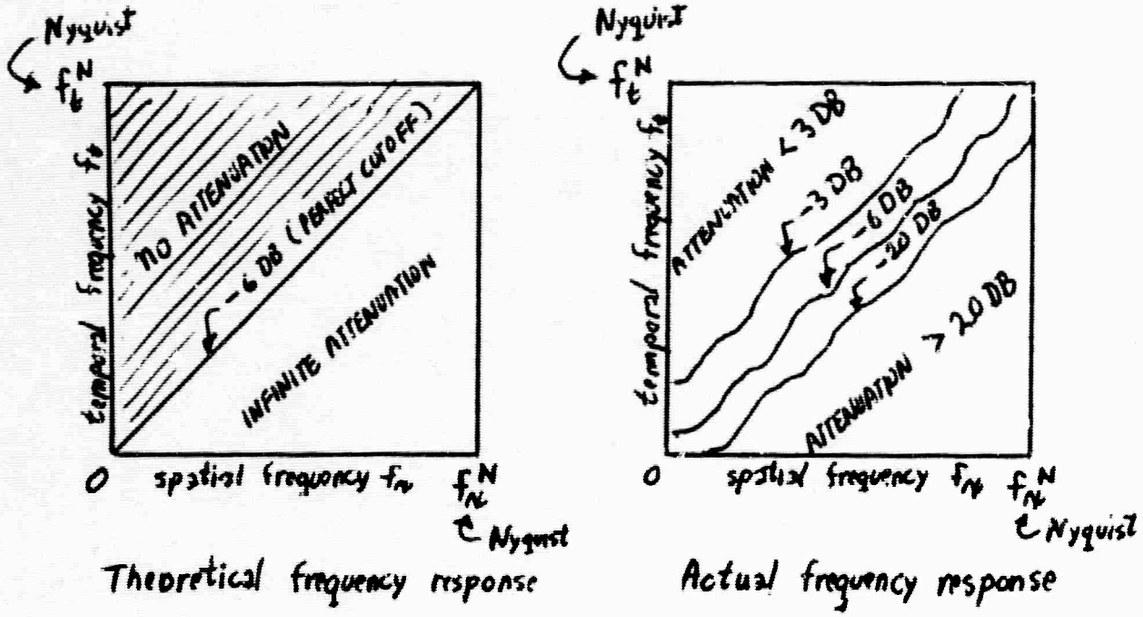

Figure 20. Theoretical vs. actual frequency response

The linear operators $Q(T_n, X_m)$ are depicted in the following diagram:

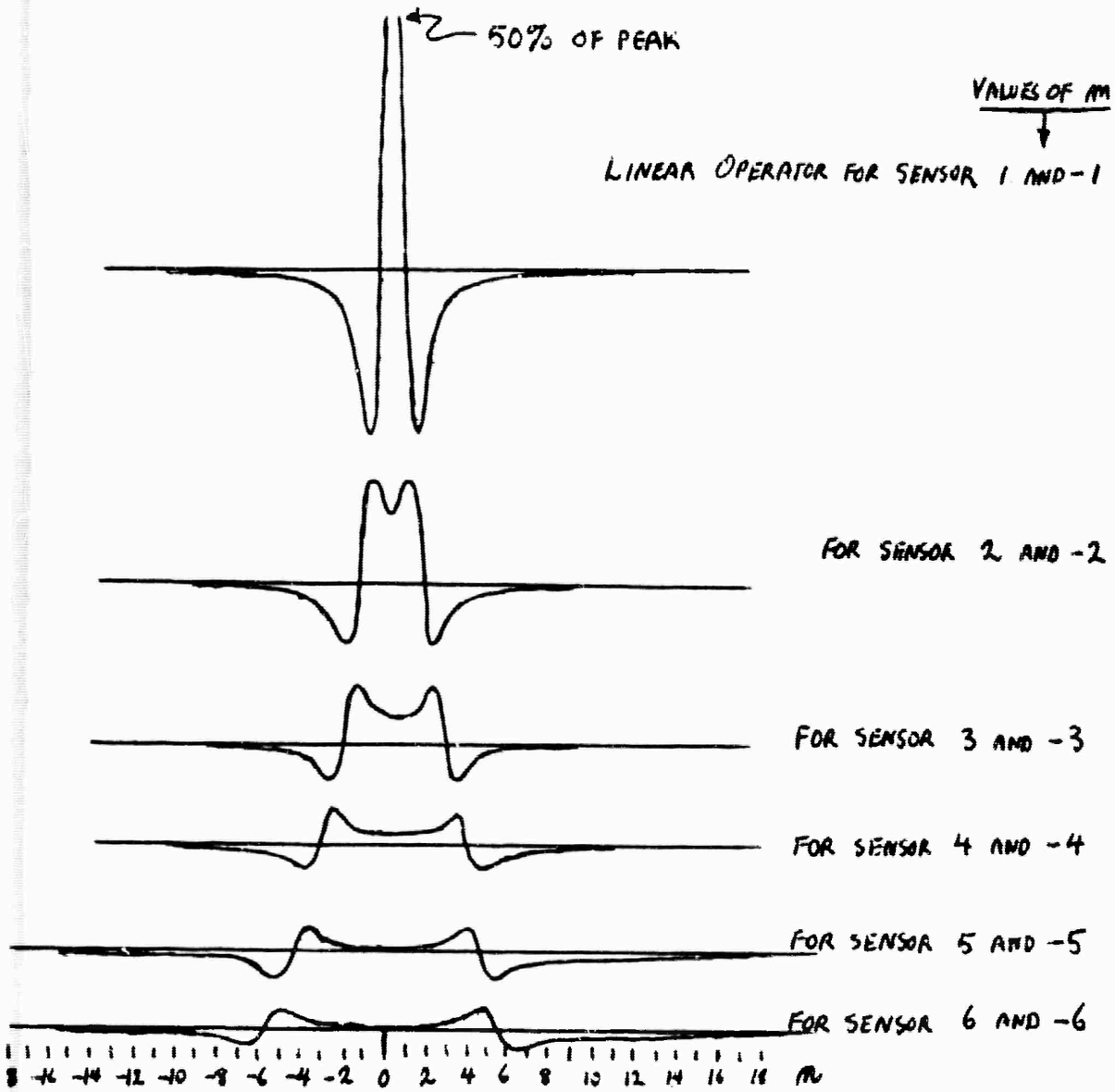

Figure 21. Linear operators for first six sensor positions

Let us now illustrate the actual process of velocity filtering. Suppose that we have the 12 traces shown in the figure:

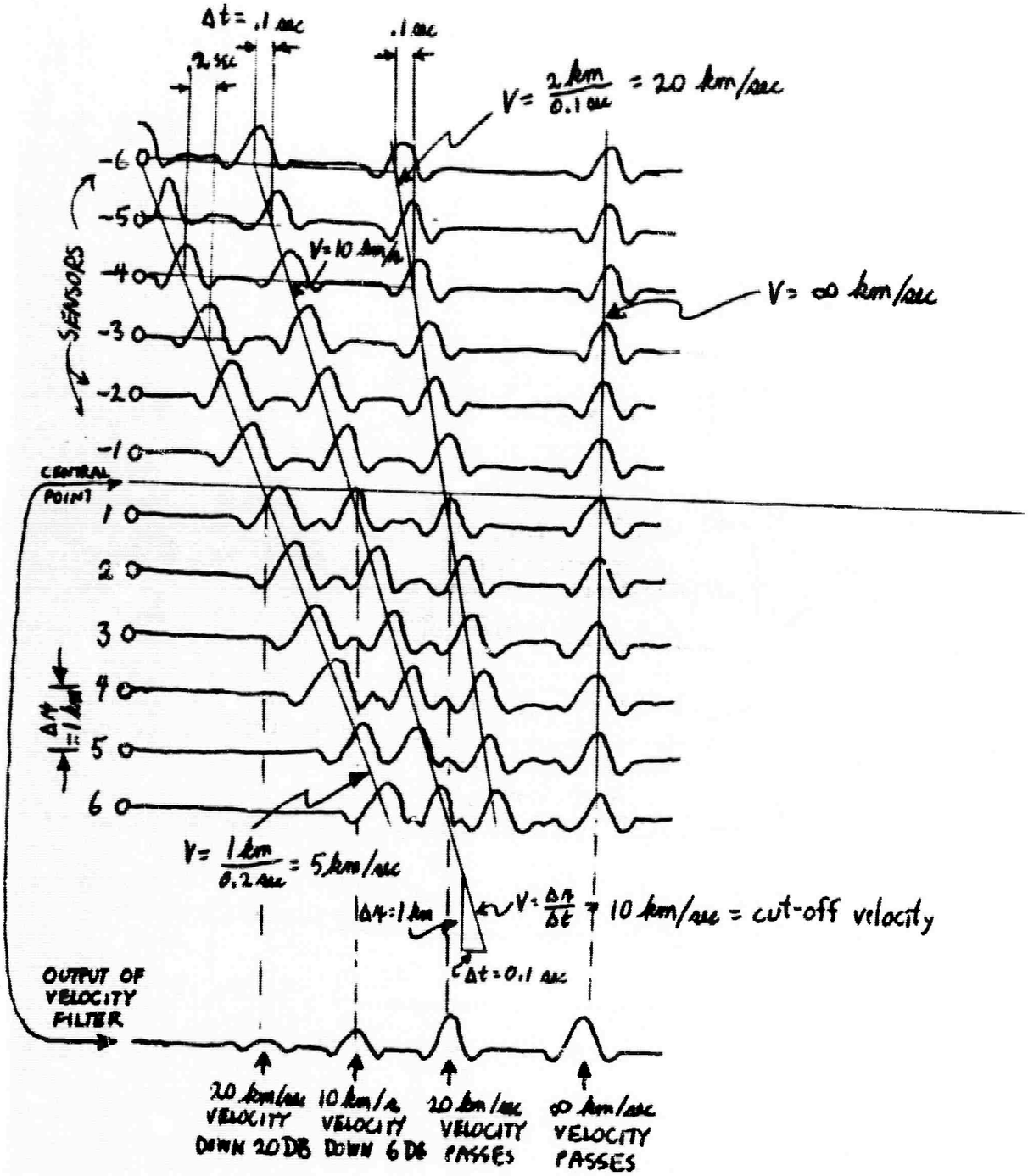

Figure 22. Effects of velocity filtering in the time-space domain

Let us choose the cut-off velocity V equal to say 10 km/sec and let us suppose the spacing of the sensors is ΔX = 1 km. Then the Nyquist spatial frequency is

$$f_x^N = \frac{1}{2\Delta X} = \frac{1}{2} \text{ c/km}$$

and the Nyquist temporal frequency is

$$f_t^N = f_x^N V = \frac{1}{2\Delta X}\frac{\Delta X}{\Delta t} = (\tfrac{1}{2})(10) = 5 \text{ c/s}$$

Hence the discrete time spacing is chosen to be

$$\Delta t = \frac{1}{2f_t^N} = \frac{1}{2(5)} = \frac{1}{10} \text{ sec} = 0.1 \text{ sec}$$

The foregoing figure portrays four events with velocities of 5 km/s, 10 km/s = the cut-off velocity, 20 km/sec, and infinite, from left to right. The waveform is a sharp transient that is identical for all events. Below the input record is the output of the velocity filter designed to pass events with a velocity greater than the cut-off velocity of 10 km/sec. The output trace corresponds to the center point of the array. Interpreting the output trace, we observe the following:

(a) Events within the pass region, that is, with velocity greater than the cut-off velocity V = 10 km/sec are passed by the process with virtually no waveform distortion.

(b) Events having a velocity equal to the cut-off velocity V = 10 km/sec are attenuated by 6 db as shown by the actual frequency response contour above, but still with virtually no waveform distortion.

(c) Events having a velocity less than the cut-off velocity are generally attenuated in amplitude by 20 db or more.

Velocity filtering offers the capability to enhance signal-to-noise ratio significantly and without danger of deteriorating signal waveform as no signal bandwidth is sacrificed. In other words, it makes it possible to process seismic array data in such a way that all seismic events with velocities in a given range are preserved with no alternation over a wide frequency band, while all seismic events with velocities outside the specified range are uniformly and severely attenuated. Velocity filtering may be looked upon as a process whereby it is possible to combine the elements of a line array in a manner resulting in a directed beam with low side lobes, where the beam width and side lobes are essentially independent of frequency. By applying the velocity filtering process to a noisy array, an output may be obtained that has all events within a specified velocity range perfectly preserved and events without this range essentially eliminated, a result which is impossible by conventional array usage.

In order to effectively utilize velocity filtering in practice, a noise and signal analysis procedure must be followed that will furnish the needed information for effective array design and emplacement. Of course, it is feasible to emplace a standard array layout at each site without prior measurement and analysis of the noise. The signal and noise parameters for the emplaced sensors would then be estimated from the actual array output, and then these parameters can be used in setting the filter responses for the processor. Thus if a standard array layout were required for political reasons, and no measurements were allowed prior to site selection, it still would be feasible to utilize the array effectively. Nevertheless, a more effective network can be established by obtaining local noise and signal characteristics and utilizing them for local optimization of the array emplacements. Thus an effective noise analysis and array design procedure can be worked out in which detailed noise measurements are made, and

a data analysis is performed to establish the temporal and spatial frequency characteristics. The necessary array length and number of sensors to provide good signal-to-noise ratios can then be determined from the noise characteristics. The performance of the array is then checked out, and it is put into production. Nevertheless, there are many complications to such a relatively straight-forward procedure.

The problem of noise measurement can be divided into three phases:

(a) Measurement of signal and noise for the purpose of selecting the site.

(b) Measurement of signal and noise at the selected site for the purpose of establishing the permanent array layout.

(c) Measurement of signal and noise on the emplaced array for the purpose of determining the necessary filter settings.

6. SPECTRAL ANALYSIS

In order to provide the desired information about the noise and signal, data analyses must be performed. It is anticipated that a real-time analysis of the data will not be possible; thus selected samples of noise and signal data are the inputs to a digital computer analysis program.

The parameters of the most importance in the design of an array are the distribution of noise and signal versus apparent horizontal propagation velocity, azimuth, spatial frequency spectrum, temporal frequency spectrum, time stability of the noise characteristics, coherence versus frequency and sensor separation. The desired information can be derived from the data by operating on the cross-correlation function and its spectral density. Also the cross-power spectra of signal and noise constitute necessary information for the design of the ideal processor. Thus the accuracy in the determination of the necessary parameters is dependent upon the accuracy with which the density spectra can be estimated, and so this problem will now be discussed in some detail.

The development of a theory of spectral analysis of empirically observed signals begins with the introduction of the notion of the sample autocorrelation function. Suppose we let

$$x_1, x_2, \cdots, x_n$$

denote the sampled values of the signal of interest. Then the sample autocorrelation is

$$\phi_n(\tau) = \begin{cases} \frac{1}{n}(x_1 x_{1+\tau} + x_2 x_{2+\tau} + \cdots + x_{n-\tau} x_n) & \text{for } \tau = 0, 1, \cdots, n-1 \\ 0 & \tau \geq n \\ \phi_n(-\tau) & \tau < 0. \end{cases}$$

The periodogram, or Fourier transform of the sample autocorrelation, is

$$\Phi_n(f) = \sum_{|\tau|<n} e^{-2\pi i f \tau} \phi_n(\tau),$$

so

$$\phi_n(\tau) = \int_{-\frac{1}{2}}^{\frac{1}{2}} e^{2\pi i \tau f} \Phi_n(f)\, df$$

The periodogram may also be written as

$$\Phi_n(f) = \phi_n(0) + 2\sum_{\tau=1}^{n-1} \cos 2\pi f \tau \cdot \phi_n(\tau)$$

and also

$$\phi_n(\tau) = 2\int_0^{\frac{1}{2}} \cos 2\pi \tau f \cdot \Phi_n(f)\, df.$$

The periodogram, like the sample autocorrelation, is an even function of its argument. For a large class of stationary processes, we have

$$\lim_{n\to\infty} \phi_n(\tau) = \phi(\tau)$$

where $\phi(\tau)$ is the autocorrelation function of the process. Then for every continuous function $G(f)$ we have

$$\lim_{n\to\infty} \int_{-\frac{1}{2}}^{\frac{1}{2}} G(f)\Phi_n(f)\, df = \lim_{n\to\infty} \int_{-\frac{1}{2}}^{\frac{1}{2}} G(f) \sum_{|\tau|<n} e^{-2\pi i \tau f} \phi_n(\tau)\, df$$

$$= \int_{-\frac{1}{2}}^{\frac{1}{2}} G(f)\left[\sum_{\tau=-\infty}^{\infty} e^{-2\pi i \tau f}\phi(\tau)\right] df$$

$$= \int_{-\frac{1}{2}}^{\frac{1}{2}} G(f)\Phi(f)\, df$$

where

$$\Phi(f) = \sum_{\tau=-\infty}^{\infty} e^{-2\pi i \tau f} \phi(\tau)$$

is the spectral density of the process. The expected value of the sample autocorrelation is

$$E\{\phi_n(\tau)\} = (1 - \frac{|\tau|}{n})\,\phi(\tau)$$

so its expected value is biased by a factor of $(1 - \frac{|\tau|}{n})$ from the true autocorrelation .

Suppose that we form a linear combination of the true autocorrelations given by

$$\sum_{\tau=-\infty}^{\infty} a_\tau \phi_\tau = \int_{-\frac{1}{2}}^{\frac{1}{2}} \left[\sum_{\tau=-\infty}^{\infty} a_\tau \cos 2\pi f \tau\right] \Phi(f)\, df .$$

Now the expression in brackets is the Fourier transform (as we assume $a_\tau = a_{-\tau}$ of the weights a_τ ; this Fourier transform is called the spectral window $A(f)$), that is

$$A(f) = \sum_{\tau=-\infty}^{\infty} a_\tau \cos 2\pi f \tau$$

Let us now assume that the stationary process is normal with zero mean. Then

$$\begin{aligned}
\mathrm{Cov}[\phi_n(t_1), \phi_n(t_2)] &= \frac{1}{n^2}\,\mathrm{Cov}\left\{\sum_{t_3} x_{t_3+t_1} x_{t_3} , \sum_{t_4} x_{t_4+t_2} x_{t_4}\right\} \\
&= \frac{1}{n^2} \sum_{t_3}\sum_{t_4} \mathrm{Cov}\left\{x_{t_3+t_1} x_{t_3} , x_{t_4+t_2} x_{t_4}\right\} \\
&= \frac{1}{n^2} \sum_{t_3}\sum_{t_4} \left\{\phi(t_3 - t_4 + t_1 - t_2)\,\phi(t_3 - t_4) + \phi(t_3 + t_1 - t_4)\,\phi(t_3 - t_4 - t_2)\right\} \\
&= \frac{1}{n} \sum_{t} \frac{U(n)}{n} \left\{\phi(t + t_1 - t_2)\,\phi(t) + \phi(t + t_1)\,\phi(t - t_2)\right\}
\end{aligned}$$

where $\frac{U(n)}{n} \longrightarrow 1$ as $n \longrightarrow \infty$. Thus as $n \longrightarrow \infty$

$$\mathrm{Cov}\left[\phi_n(t_1), \phi_n(t_2)\right] \rightarrow \frac{1}{n} \sum_t \left\{\phi(t+t_1-t_2)\phi(t) + \phi(t+t_1)\phi(t-t_2)\right\}$$

$$= \frac{1}{n} \int_{-\frac{1}{2}}^{\frac{1}{2}} \Phi^2(f)\left[e^{2\pi i f(t_1-t_2)} + e^{2\pi i f(t_1+t_2)}\right] df$$

But

$$e^{2\pi i f(t_1-t_2)} + e^{2\pi i f(t_1+t_2)} = e^{2\pi i f t_1}\left(e^{2\pi i f t_2} + e^{-2\pi i f t_2}\right)$$

$$= e^{2\pi i f t_1}\, 2\cos(2\pi f t_2)$$

Hence

$$\mathrm{Cov}\left[\phi_n(t_1), \phi_n(t_2)\right] \rightarrow \frac{1}{n} \int_{-\frac{1}{2}}^{\frac{1}{2}} \Phi^2(f)\, e^{2\pi i f t_1}\, 2\cos(2\pi f t_2)\, df$$

$$= \frac{2}{n} \int_{-\frac{1}{2}}^{\frac{1}{2}} \Phi^2(f)\cos(2\pi f t_1)\cos(2\pi f t_2)\, df$$

as $n \longrightarrow \omega$.

Thus the deviations of the sample autocorrelation from the true autocorrelation

$$\delta_n(\tau) = \phi_n(\tau) - \phi(\tau) \qquad \tau = 0, \pm 1, \pm 2, \cdots$$

is approximately normal with means

$$E\left\{\delta_n(\tau)\right\} = E\left\{\phi_n(\tau)\right\} - \phi(\tau) = \left(1 - \frac{|\tau|}{n}\right)\phi(\tau) - \phi(\tau)$$

$$= -\frac{|\tau|}{n}\phi(\tau) \rightarrow 0 \qquad \text{as} \quad n \longrightarrow \infty$$

and covariances

$$\operatorname{Cov}\left\{\delta_n(t_1), \delta_n(t_2)\right\} \doteq \operatorname{Cov}\left\{\phi_n(t_1), \phi_n(t_2)\right\}$$

$$\to \frac{2}{n}\int_{-\frac{1}{2}}^{\frac{1}{2}} \Phi^2(f) \cos 2\pi f t_1 \cos 2\pi f t_2 \, df$$

as $n \to \infty$.

The spectral band power estimate is an estimate of the spectral mass in the interval (f_0-h, f_0+h) which is

$$\int_{f_0-h}^{f_0+h} \Phi(f)\, df = \frac{1}{2}\left[\int_{-f_0-h}^{-f_0+h} \Phi(f)\, df + \int_{f_0-h}^{f_0+h} \Phi(f)\, df\right].$$

The spectral window is

$$A(f) = \begin{cases} \frac{1}{2} & \text{for } -f_0-h \le f \le -f_0+h \\ \frac{1}{2} & \text{for } f_0-h \le f \le f_0+h \\ 0 & \text{otherwise} \end{cases}$$

which is an even function of f. The corresponding weights are

$$a_t = \int_{-\frac{1}{2}}^{\frac{1}{2}} A(f) e^{2\pi i f t}\, df = 2\int_0^{\frac{1}{2}} A(f) \cos 2\pi f t \, df$$

$$= \int_{f_0-h}^{f_0+h} \cos 2\pi f t \, df = \frac{\sin 2\pi f t}{2\pi t}\Bigg]_{f=f_0-h}^{f=f_0+h}$$

$$= \frac{\sin 2\pi(f_0+h)t - \sin 2\pi(f_0-h)t}{2\pi t} = \frac{1}{\pi t}\cos 2\pi f_0 t \sin 2\pi h t$$

Thus, in order to estimate

$$\sum_{t=-\infty}^{\infty} a_t \phi(t) = \int_{-\frac{1}{2}}^{\frac{1}{2}} A(f)\, \Phi(f)\, df = \int_{f_0-h}^{f_0+h} \Phi(f)\, df$$

we could use the estimate (the spectral band power estimate)

$$\sum_{|t|<n} a_t \phi_n(t) = \int_{-\frac{1}{2}}^{\frac{1}{2}} A(f)\, \Phi_n(f)\, df$$

and since $\phi_n(t) = 0$ for $|t| \geq n$ this estimate can be written

$$\sum_{t=-\infty}^{\infty} a_t \phi_n(t) = \int_{-\frac{1}{2}}^{\frac{1}{2}} A(f)\, \Phi_n(f)\, df = \int_{f_0-h}^{f_0+h} \Phi_n(f)\, df.$$

In other words, the spectral band power estimate is equal to the energy in the periodogram in the spectral band of interest. The expected value of this estimate is

$$\begin{aligned} E\left\{\sum_{t=-\infty}^{\infty} a_t \phi_n(t)\right\} &= \sum_{t=-\infty}^{\infty} a_t\, E\{\phi_n(t)\} \\ &= \sum_{|t|<n} a_t \left(1-\frac{|t|}{n}\right) \phi_n(t) \\ &= \sum_{t=-\infty}^{\infty} a_t\, w_t\, \phi_n(t). \end{aligned}$$

Now the function defined by

$$w_t = \begin{cases} 1-\frac{|t|}{n} & \text{for } |t|<n \\ 0 & \text{for } |t| \geq n \end{cases}$$

serves as a weighting function to improve the convergence of

$$\sum_{|t|<n} a_t \cos 2\pi f t$$

to $A(f)$ as $n \to \infty$. In other words

$$\sum_{|t|<n} a_t w_t \cos 2\pi f t$$

is a better approximation to $A(f)$. The weighting function w_t just given is the well-known Fejer weighting function; of course, any number of other choices are possible.

For example, suppose we estimate the autocorrelation by

$$\phi_n(\tau) = \begin{cases} \frac{1}{m}(x_1 x_{1+\tau} + x_2 x_{2+\tau} + \cdots + x_m x_{m+\tau}) & \text{for } \tau = 0, 1, \cdots, m, \\ 0 & \text{for } \tau > n, \\ \phi_n(-\tau) & \text{for } \tau < 0. \end{cases}$$

Then

$$E\{\phi_n(\tau)\} = \begin{cases} \phi(\tau) & \text{for } |\tau| = 0, 1, \cdots, n, \\ 0 & \text{for } |\tau| > n, \end{cases}$$

so the expected value of the spectral band estimate is

$$E\left\{\sum_{t=-\infty}^{\infty} a_t \phi_n(t)\right\} = \sum_{|t|\le n_1} a_t \phi_n(t) = \sum_{t=-\infty}^{\infty} a_t w_t \phi_n(t)$$

where

$$w_t = \begin{cases} 1 & \text{for } |t| \le n_1 \\ 0 & \text{for } |t| > n_1. \end{cases}$$

This is the well-known Dirichlet weighting function.

The statistic $\sum_{|t|<n} a_t \phi_n(t)$ under the stated conditions is normal with mean

$$\sum_{|t|<n} a_t w_t \phi(t) = \int_{-\frac{1}{2}}^{\frac{1}{2}} \left[\sum_{|t|<n} a_t w_t \cos 2\pi f t \right] \Phi(f)\, df$$

and variance

$$\sum_{|t_1|<n} \sum_{|t_2|<n} a_{t_1} a_{t_2} \operatorname{Cov}\left[\phi_n(t_1), \phi_n(t_2)\right]$$

$$\doteq \sum_{|t_1|<n} \sum_{|t_2|<n} a_{t_1} a_{t_2} \frac{2}{n} \int_{-\frac{1}{2}}^{\frac{1}{2}} \Phi^2(f) \cos 2\pi f t_1 \cos 2\pi f t_2\, df$$

$$\doteq \frac{2}{n} \int_{-\frac{1}{2}}^{\frac{1}{2}} \left(\sum_{|t_1|<n} a_{t_1} \cos 2\pi f t_1 \right) \left(\sum_{|t_2|<n} a_{t_2} \cos 2\pi f t_2 \right) \Phi^2(f)\, df$$

$$\to \frac{2}{n} \int_{-\frac{1}{2}}^{\frac{1}{2}} \left[A(f) \Phi(f) \right]^2 df \qquad \text{as } n \to \infty$$

Thus the above statistic suffers from two kinds of errors. One, the bias comes up because the mean of the statistic is not equal to

$$\sum_{t=-\infty}^{\infty} a_t \phi_t = \int_{-\frac{1}{2}}^{\frac{1}{2}} A(f) \Phi(f)\, df$$

but is equal to

$$\sum_{|t|<n} Q_t w_t \phi(t) = \int_{-\frac{1}{2}}^{\frac{1}{2}} \left[\sum_{|t|<n} Q_t w_t \cos 2\pi f t \right] \Phi(f)\, df .$$

The other error, due to statistical fluctuations, is indicated by the variance

$$\frac{2}{n} \int_{-\frac{1}{2}}^{\frac{1}{2}} \left[\sum_{|t|<n} Q_t \cos 2\pi f t \right]^2 \Phi^2(f)\, df .$$

Further discussion of these points is given in the work of Parzen (1961, 1964) and Blackman and Tukey (1958).

7. DISCUSSION OF SPECTRAL WINDOWS

As we have seen, narrow time signals have spectra that are wide, and conversely. In order to give a quantitative measure to this observation, we need to define the durations of a signal and its Fourier transform in a simple and useful way, but no single definition can be suitable for all possible signals.

For a measure of the duration of a time signal $g(t)$ the second moment of $|g(t)|^2$ about its mean or some other suitably chosen point can be used, which we can take to be the origin $t=0$. From $g(t) \leftrightarrow G(f)$ we obtain the Fourier transform pair

$$-2\pi i t\, g(t) \leftrightarrow \frac{dG(f)}{df} = \left(\frac{dA}{df} + iA\frac{d\phi}{df}\right) e^{i\phi}$$

where $G(f) = A(f)e^{i\phi(f)}$. By Parseval's formula we have

$$(2\pi)^2 \int_{-\infty}^{\infty} t^2 |g(t)|^2 dt = \int_{-\infty}^{\infty} \left|\frac{dG}{df}\right|^2 df$$

$$= \int_{-\infty}^{\infty} \left[\left(\frac{dA}{df}\right)^2 + A^2\left(\frac{d\phi}{df}\right)^2\right] df.$$

We therefore conclude that high ripple in the amplitude A or phase ϕ results in signals of long time duration. Among all functions with the same amplitude $A(\omega)$ the minimum phase one has the shortest time duration.

To simplify notation, let us assume that the energy of the signals under consideration equals one:

$$\int_{-\infty}^{\infty} |g(t)|^2 dt = \int_{-\infty}^{\infty} A^2(f)\, df = 1.$$

The Schwarz inequality is

$$\left| \int_{-\infty}^{\infty} g_1 g_2 \, dt \right|^2 \leq \int_{-\infty}^{\infty} |g_1|^2 dt \int_{-\infty}^{\infty} |g_2|^2 dt$$

where the two sides are equal only if g_1 is proportional to g_2. Let us insert into this inequality the functions

$$g_1(t) = t\, g(t), \quad g_2(t) = \frac{dg(t)}{dt}.$$

Hence

$$\left| \int_{-\infty}^{\infty} t g \frac{dg}{dt} dt \right|^2 \leq \int_{-\infty}^{\infty} |tg|^2 dt \int_{-\infty}^{\infty} \left| \frac{dg}{dt} \right|^2 dt.$$

Integrating the left hand side integral by parts we have

$$\int_{-\infty}^{\infty} t g \frac{dg}{dt} dt = t \frac{g^2}{2} \Big]_{-\infty}^{\infty} - \frac{1}{2} \int_{-\infty}^{\infty} g^2 dt = -\frac{1}{2}$$

where we have assumed g is real and $tg \to 0$ as $t \to \pm\infty$. From $\frac{dg}{dt} \leftrightarrow 2\pi i f G(f)$ it follows that

$$\int_{-\infty}^{\infty} \left(\frac{dg}{dt} \right)^2 dt = \int_{-\infty}^{\infty} [2\pi f A(f)]^2 df.$$

Hence

$$\frac{1}{4} \leqslant \int_{-\infty}^{\infty} t^2 g^2 \, dt \int_{-\infty}^{\infty} (2\pi f)^2 A^2(f) \, df$$

If we let $\beta^2 = \int_{-\infty}^{\infty} t^2 g^2 \, dt$ and $\alpha^2 = \int_{-\infty}^{\infty} (2\pi f)^2 A^2(f) \, df$ then we have $\beta^2 \alpha^2 \geqslant \frac{1}{4}$.

The equality sign holds if $\frac{dg}{dt} = k t g(t)$ where k is a constant. Solving, we obtain

$$g(t) = C e^{k\frac{t^2}{2}}$$

Choosing $k = -\frac{1}{2\beta^2} = -2\alpha^2$ we obtain

$$g(t) = C e^{-\frac{t^2}{4\beta^2}}$$

The transform of $g(t)$ is

$$G(f) = C\sqrt{2}\beta\sqrt{2\pi}\, e^{-\frac{1}{2}2\beta^2(2\pi f)^2} = \sqrt{2}\beta C\sqrt{2\pi}\, e^{-\frac{(2\pi f)^2}{4\alpha^2}}$$

Thus a narrow pulse $g(t)$ has a wide spectrum $G(f)$, and conversely. This pulse $g(t)$ is the well-known Gaussian pulse.

Another set of well-known pulses are:

$$g(t) = \begin{cases} \cos^n \frac{\pi t}{\tau} & \text{for } -\frac{\tau}{2} \leqslant t \leqslant \frac{\tau}{2} \\ 0 & \text{Otherwise} \end{cases}$$

for various values of n . These are called the <u>nth power cosine</u> pulses. The transform of $g(t)$ is

$$G(f) = \int_{-\frac{\tau}{2}}^{\frac{\tau}{2}} \cos^n \frac{\pi t}{\tau}\, e^{-2\pi i f t} \, dt.$$

Let us choose our units so $\tau = 2$, so

$$g(t) = \begin{cases} \cos^n \frac{\pi t}{2} & \text{for } |t| \le 1 \\ 0 & \text{for } |t| > 1. \end{cases}$$

Then

$$G(f) = \int_{-1}^{1} \cos^n \frac{\pi t}{2}\, e^{-2\pi i f t}\, dt$$

$$= 2 \int_{0}^{1} \cos^n \frac{\pi t}{2} \cos 2\pi f t\, dt$$

$$= \frac{4}{\pi} \frac{n! \cos 2\pi f}{\prod_{k=0}^{\frac{n-1}{2}} [(2k+1)^2 - 16f^2]} \quad \text{when } n = 1,3,5,7,\cdots$$

$$= 2 \frac{n!}{\prod_{k=1}^{\frac{n}{2}} [(2k)^2 - 16f^2]} \frac{\sin 2\pi f}{2\pi f} \quad \text{when } n = 2,4,6,\cdots$$

For example, if $n=1$ then

$$g(t) = \cos\frac{\pi t}{2} \qquad \text{for } |t| \le 1$$

and

$$G(f) = \frac{4}{\pi}\,\frac{\cos 2\pi f}{1-16f^2} \qquad (\text{case } \tau = 2).$$

If on the other hand we had let $\tau = 1$ (and $n=1$) then

$$g(t) = \begin{cases} \cos \pi t & |t| \le \frac{1}{2} \\ 0 & |t| > \frac{1}{2} \end{cases}$$

and

$$G(f) = \int_{-\frac{1}{2}}^{\frac{1}{2}} \cos \pi t \cos 2\pi f t \, dt$$

Letting $t' = 2t$ we have

$$G(f) = \frac{1}{2}\int_{-1}^{1} \cos\frac{\pi t'}{2} \cos 2\pi f \frac{t'}{2} \, dt'$$

$$= \frac{1}{2}\int_{-1}^{1} \cos\frac{\pi t'}{2} \cos 2\pi \frac{f}{2} t' \, dt'$$

$$= \frac{1}{2}\,\frac{4}{\pi}\,\frac{\cos 2\pi \frac{f}{2}}{1-16(\frac{f}{2})^2}$$

from the foregoing result.

Hence

$$G(f) = \frac{2}{\pi} \frac{\cos \pi f}{1 - 4f^2} \qquad (\text{for case } \tau = 1)$$

Now suppose $n = 2$. Then

$$g(t) = \begin{cases} \cos^2 \frac{\pi t}{\tau} = \frac{1}{2} + \frac{1}{2} \cos \frac{2\pi t}{\tau} & \text{for } |t| \leq \frac{\tau}{2} \\ 0 & \text{for } |t| > \frac{\tau}{2}. \end{cases}$$

This is the well-known pulse named after the Austrian meteorologist Julius von Hann, and called "hanning" by Blackman and Tukey (1958).

If we let $\frac{\tau}{2} = T$, then the von Hann pulse becomes

$$g(t) = \frac{1}{2}(1 + \cos \frac{\pi t}{T}) \qquad \text{for } |t| \leq T$$

Now $g(t)$ may be written

$$g(t) = \frac{1}{2}(1 + \frac{1}{2} e^{i\frac{\pi t}{T}} + \frac{1}{2} e^{-i\frac{\pi t}{T}}) \operatorname{rect}(t)$$

where $\operatorname{rect}(t)$, read "rectangle of t " is defined as

$$g_R(t) = \operatorname{rect}(t) = \begin{cases} 1 & \text{for } |t| \leq T \\ 0 & \text{for } |t| > T. \end{cases}$$

The transform of $\operatorname{rect}(t)$ is

$$G_R(f) = \operatorname{RECT}(f) = \int_{-T}^{T} \cos 2\pi f t \, dt = 2T \frac{\sin 2\pi f T}{2\pi f T}.$$

Hence the transform of $g(t)$ is

$$G(f) = \left[\frac{1}{2}\left(\delta(f) + \frac{1}{2}\delta\left(f+\frac{1}{2T}\right) + \frac{1}{2}\delta\left(f-\frac{1}{2T}\right)\right)\right] * \left[2T\,\frac{\sin 2\pi fT}{2\pi fT}\right]$$

$$= \frac{1}{2}\,\frac{\sin 2\pi fT}{\pi f} + \frac{1}{4}\,\frac{\sin 2\pi\left(f+\frac{1}{2T}\right)T}{\pi\left(f+\frac{1}{2T}\right)} + \frac{1}{4}\,\frac{\sin 2\pi\left(f-\frac{1}{2T}\right)T}{\pi\left(f-\frac{1}{2T}\right)}$$

$$= \frac{\sin 2\pi fT}{2}\left[\frac{1}{\pi f} - \frac{1}{2\pi\left(f+\frac{1}{2T}\right)} - \frac{1}{2\pi\left(f-\frac{1}{2T}\right)}\right]$$

$$= \frac{\sin 2\pi fT}{2}\left[\frac{1}{\pi f} - \frac{2\pi f - \frac{\pi}{T} + 2\pi f + \frac{\pi}{T}}{(2\pi f)^2 - \left(\frac{\pi}{T}\right)^2}\right]$$

$$= \frac{\sin 2\pi fT}{2}\left[\frac{(2\pi f)^2 - \left(\frac{\pi}{T}\right)^2 - (2\pi f)^2}{\pi f\left[(2\pi f)^2 - \left(\frac{\pi}{T}\right)^2\right]}\right]$$

$$= \sin 2\pi fT\;\frac{-\frac{\pi^2}{T^2}}{2\pi f\left[(2\pi f)^2 - \left(\frac{\pi}{T}\right)^2\right]}$$

$$= \frac{\sin 2\pi fT}{2\pi fT} \cdot \left(\pi^2 T\right)\,\frac{1}{\pi^2 - (2\pi fT)^2}$$

If we let $\alpha = 2\pi fT$, then

$$G(f) = \pi^2 T\,\frac{\sin\alpha}{\alpha}\,\frac{1}{\pi^2 - \alpha^2}.$$

The spectrum $G(f)$ is thus the $\frac{\sin\alpha}{\alpha}$ function, corresponding to a uniform aperture distribution, multiplied by $\pi^2 T$ times the factor $\frac{1}{\pi^2-\alpha^2}$. When $\alpha = \pm\pi$, this factor is infinite, but $G(f)$ remains finite since $\sin\alpha$ also vanishes at $\alpha = \pm\pi$. The first zeros of $\frac{\sin\alpha}{\alpha}$ are thus suppressed. For increasing values of $|\alpha|$, greater than π, the factor $\frac{1}{\pi^2-\alpha^2}$ decreases rapidly, thus reducing the intensity of the side lobes. This is of course why a cosine-squared pulse is used in preference to the rectangular pulse in spectral estimation. The following figure shows $G_R(f)$ for the rectangular pulse $g_R(t) = 1$ for $|t| \leq T$ and $= 0$ for $|t| > T$ and the cosine-squared pulse:

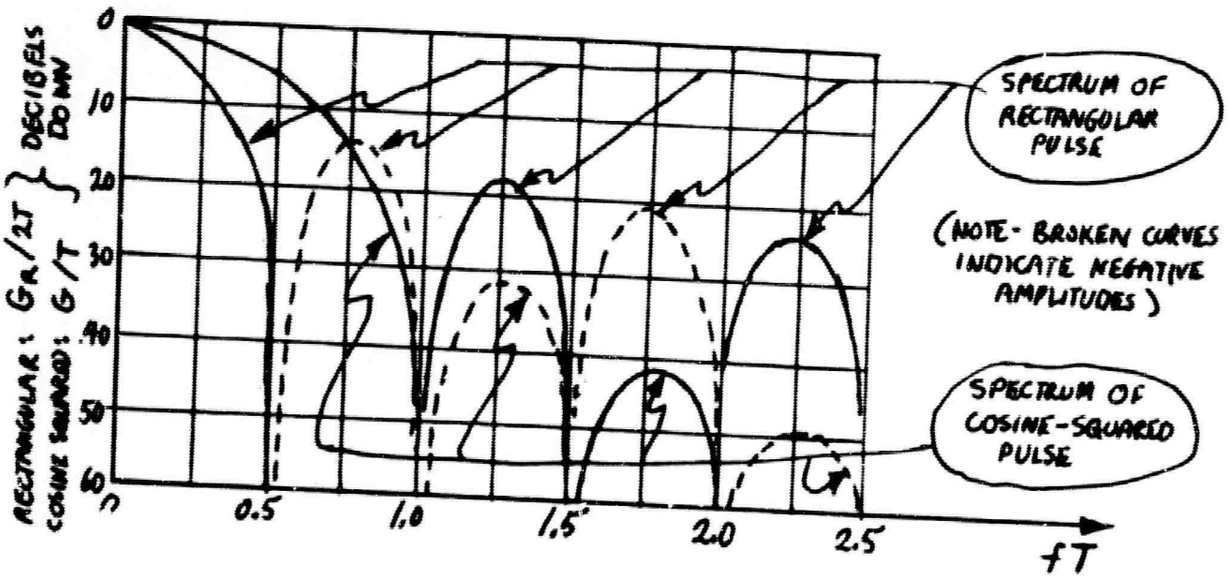

Figure 23. Spectra of rectangular and cosine-squared pulses

8. RELATIONSHIP BETWEEN CONTINUOUS AND DISCRETE APERTURE FUNCTIONS

Suppose that we have an array of equidistant elements ($\Delta x_k' = d$) connected in phase with weighting $T(x_k') = T(x_{-k}') = T_k$. See figure 24.

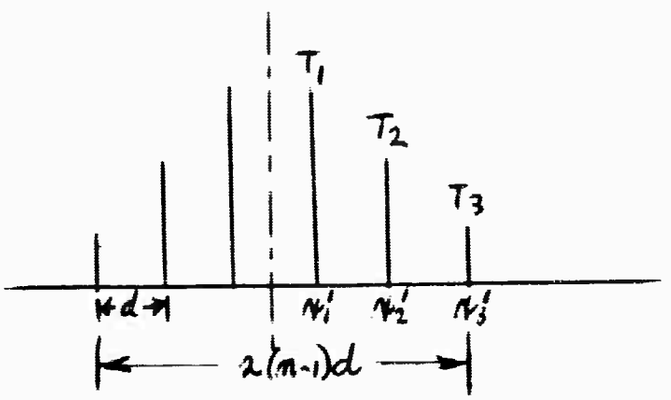

Figure 24. A six-element array

We shall only discuss the symmetrical array consisting of $2n$ elements; a similar theory can be developed for an odd number of elements.

The pattern of this type of array as a function of direction θ is given by

$$\left| A_{2n}(\theta) \right| = 2 \left| \sum_{k=1}^{n} T_k \cos \frac{2\pi x_k' \sin\theta}{\lambda} \right|$$

Let us indroduce the new variables

$$x_k = \frac{x_k'}{2nd} = \frac{(k-\frac{1}{2})d}{2nd} = (k-\tfrac{1}{2})\frac{1}{2n} \quad \text{for } k = 1, 2, \cdots, n$$

and

$$\xi = \frac{\sin\theta}{\frac{\lambda}{2nd}} .$$

Then we have

$$|A_{2n}(\xi)| = 2\left|\sum_{k=1}^{n} T_k \cos 2\pi x_k \xi\right|$$

$$= 2\left|\sum_{k=1}^{n} T_k \cos(2k-1)\frac{\pi\xi}{2n}\right| .$$

The function $|A_{2n}(\xi)|$ is periodic with period $2n$.

Let us now consider a continuous aperture function $T_c(x)$ of width $L = 2nd$ passing through the points (x_k, T_k) of the array. The pattern due to this continuous function is

$$A_c(\xi) = \int_{-\frac{1}{2}}^{\frac{1}{2}} T_c(x) \cos 2\pi x\xi \, dx$$

in comparison to the pattern of the array, which we recall was

$$A_{2n}(\xi) = 2\sum_{k=1}^{n} T_k \cos 2\pi x_k \xi .$$

In order to show the relation between $A_{2n}(\xi)$ and $A_c(\xi)$, we represent the array T_k as the product of $T_c(x)$ with a uniform array of infinite extent and reduced interval $1/2n$:

$$T_k = \mathrm{comb}_{\frac{1}{2n}} \cdot T_c(x) .$$

Here we use the notation

$$\text{comb}_F\, U(x) = \sum_{k=-\infty}^{\infty} U(kx)\,\delta(x-kF).$$

See Figure 25:

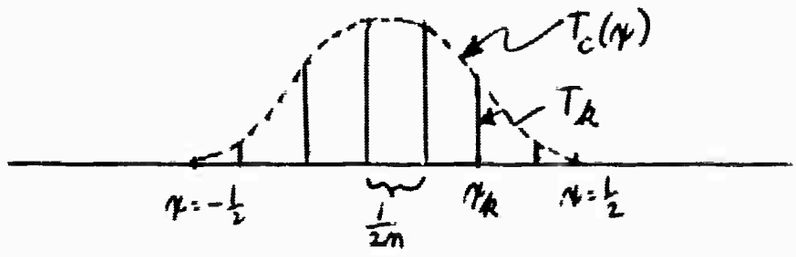

Figure 25. T_k as the product of $T_c(x)$ with a comb function

As a result, the spectrum of T_k is the convolution of the spectra of $\text{comb}_{\frac{1}{2n}}$ and $T_c(x)$. Because the spectrum of $\text{comb}_{\frac{1}{2n}}$ is another uniform array of infinite extent with period $2n\,(=L/d)$ we have

$$A_{2n}(\xi) = \text{comb}_{2n} * A_c(\xi)$$

or

$$A_{2n}(\xi) = \sum_{k=-\infty}^{\infty} A_c(\xi+2nk) = \text{rep}_{2n} A_c(\xi)$$

where rep is defined by

$$\mathrm{rep}_T\, u(t) = \sum_{k=-\infty}^{\infty} u(t+kT).$$

This is the well-known result of aliasing (Blackman and Tukey, 1958; Jacquinot and Roizen-Dossier, 1964).

9. LISTING OF VARIOUS APERTURE FUNCTIONS AND THEIR WINDOWS

The form of an aperture function is indeterminate to the extent of a proportionality factor. In order to compare different functions some convention must be chosen to fix this factor. We suppose that the real aperture function $g(x)$ vanishes outside the interval $-1/2 \leq x \leq 1/2$. We want the function to have the maximum possible transmission. Because the intensity at the center of the pattern produced by the uniform aperture function $g_0(x) = 1$ for $-1/2 \leq x \leq 1/2$ is

$$I_0(0) = \left[G_0(0)\right]^2 = \left[\int_{-\frac{1}{2}}^{\frac{1}{2}} dx\right]^2 = 1,$$

we shall consider in the case of a non-uniform aperture function the ratio

$$\frac{I(0)}{I_0(0)} = \left[\frac{G(0)}{G_0(0)}\right]^2 = \left[\int_{-\frac{1}{2}}^{\frac{1}{2}} g(x)\,dx\right]^2.$$

We wish to decrease side-lobes as much as possible without decreasing $I(0)/I_0(0)$ too much.

The total energy transmitted by the aperture is proportional to

$$\tau = \int_{-\frac{1}{2}}^{\frac{1}{2}} \left[g(x)\right]^2 dx$$

which for a uniform aperture function is

$$\tau_0 = 1.$$

Therefore we are concerned by the ratio

$$\frac{\tau}{\tau_0} = \int_{-\frac{1}{2}}^{\frac{1}{2}} \left[g(x)\right]^2 dx.$$

Our object must be to decrease the side-lobe level without decreasing τ/τ_0 too much.

The width of the main lobe of the pattern $G(\theta)$ is also of interest. Let us as a convention put the width $\Delta\ell_0$ of the main lobe of the pattern from the uniform aperture function equal to unity; this unit width turns out to be the distance between the two points with ordinate 0.405. We then extend this definition to other patterns; their widths $\Delta\ell$ will be taken always to be the distance between points of the normalized ordinate 0.405.

To confirm our notation in this section, we have:

$$\underline{\text{Aperture}} \quad : \quad g(x) = \begin{cases} \text{real function of } x & \text{for } |x| \le \frac{1}{2} \\ 0 & \text{for } |x| > \frac{1}{2} \end{cases}$$

$$\underline{\text{Pattern}} \text{ (or } \underline{\text{window}}) \quad : \quad G(\theta) = \int_{-\frac{1}{2}}^{\frac{1}{2}} g(x)\, e^{-2\pi i x\theta}\, dx$$

$$\text{Intensity} \quad : \quad I(\theta) = |G(\theta)|^2$$

Zero subscripts refer to the uniform aperture function $g_0(x) = 1$ for $|x| \le \frac{1}{2}$. It turns out also that all the aperture functions we consider are even functions of x so $G(\theta)$ is real.

1. Triangular aperture: $g(x) = 1 - |2x|$

$$\frac{I(\theta)}{I(0)} = \frac{\sin^4 \frac{1}{2}\pi\theta}{(\frac{1}{2}\pi\theta)^4}$$

$$\frac{\tau}{\tau_0} = 0.33 \;, \qquad \frac{I(0)}{I_0(0)} = 0.25 \;, \qquad \frac{\Delta l}{\Delta l_0} = 1.46$$

---

2. Sinus cardinal aperture: $g(x) = \frac{\sin 2\pi x}{2\pi x}$

$$\frac{I(\theta)}{I(0)} = \left[\frac{Si\,\pi(\theta+1) - Si\,\pi(\theta-1)}{2\,Si\,\pi} \right]^2$$

$$\frac{\tau}{\tau_0} = \frac{Si\,2\pi}{\pi} = 0.45, \quad \frac{I(0)}{I_0(0)} = \left(\frac{Si\,\pi}{\pi}\right)^2 = 0.35, \quad \frac{\Delta l}{\Delta l_0} = 1.42$$

---

3. Cosine aperture: $g(x) = \cos \pi x$

$$\frac{I(\theta)}{I(0)} = \frac{\cos^2 \pi\theta}{(1-4\theta^2)^2}$$

$$\frac{\tau}{\tau_0} = 0.5, \qquad \frac{I(0)}{I_0(0)} = \frac{4}{\pi^2} = 0.40, \qquad \frac{\Delta l}{\Delta l_0} = 1.34$$

---

4. Gaussian aperture: $g(x) = e^{-16x^2}$

$$\frac{I(\theta)}{I(0)} = \left[e^{-\frac{1}{16}\pi^2\theta^2} \right]^2$$

(Note: This $I(\theta)/I(0)$ does not represent the intensity exactly, as it neglects the cut-off of $g(x)$ at $x = \pm 1/2$.)

$$\frac{\tau}{\tau_0} = \sqrt{\frac{\pi}{32}} = 0.31, \qquad \frac{I(0)}{I_0(0)} = 0.19, \qquad \frac{\Delta l}{\Delta l_0} = 1.72$$

---

5. $(1-4x^2)^{3/2}$ aperture: $g(x) = (1-4x^2)^{3/2}$

$$\frac{I(\theta)}{I(0)} = \left\{ \frac{8 J_2(\pi\theta)}{\pi^2\theta^2} \right\}^2$$

$$\frac{\tau}{\tau_0} = 0.45, \qquad \frac{I(0)}{I_0(0)} = \left(\frac{3\pi}{16}\right)^2 = 0.34, \qquad \frac{\Delta l}{\Delta l_0} = 1.43$$

---

6. $(1-4x^2)^2$ aperture: $g(x) = (1-4x^2)^2$

$$\frac{I(\theta)}{I(0)} = \left[\Lambda_{\frac{5}{2}}(\theta) \right]^2 = \left[15\sqrt{\frac{\pi}{2}} \frac{J_{\frac{5}{2}}(\pi\theta)}{(\pi\theta)^{\frac{5}{2}}} \right]^2$$

$$\frac{\tau}{\tau_0} = 0.41, \qquad \frac{I(0)}{I_0(0)} = 0.28, \qquad \frac{\Delta l}{\Delta l_0} = 1.54$$

Note: Here $\Lambda_\nu(\theta) = 2^\nu \Gamma(\nu+1) \frac{J_\nu(\pi\theta)}{(\pi\theta)^\nu}$ where J_ν is Bessel function of order ν.

7. $(1-4x^2)^\nu$ aperture: $g_\nu(x) = (1-4x^2)^\nu$ for $\nu \geq 0$

$$G_\nu(\theta) = \frac{\sqrt{\pi}}{2} \frac{\Gamma(\nu+1)}{\Gamma(\nu+\frac{3}{2})} \Lambda_{\nu+\frac{1}{2}}(\theta)$$

10. REFERENCES

Ahiezer, N. I. and M. Krein, 1962, Theory of Moments, American Math. Society, Providence.

Barber, N. F., 1961, Experimental Correlograms and Fourier Transforms, Pergamon Press, London, p. 136.

Beckmann, P. and A. Spizzichino, 1963, The Scattering of Electromagnetic Waves from Rough Surfaces, Pergamon Press, London, p.503.

Blackmann, R. B. and J. W. Tukey, 1958, The Measurement of Power Spectra, Dover, New York.

Brown, W. M., 1963, Analysis of Time-invariant Systems, McGraw-Hill, New York, p. 339.

Embree, P., J. P. Burg and M. M. Backus, 1963, Wide band velocity filtering, Geophysics, vol. 28, pp. 948-974.

Fail, M. D. and G. Grau, 1963, Les filtres en eventail, Geophysical Prospecting, vol. 11, pp. 131-163.

Geronimus, Ya. L., 1960, Polynomials Orthogonal on a Circle and Interval, Pergamon Press, London, p. 210.

Jacquinot and Roizen-Dossier, 1964, Apodization, Progress in Optics, vol. 3, North-Holland Publishing Co., Amsterdam.

Parzen, E., 1961, Mathematical considerations in the estimation of spectra, Technometrics, vol. 3, pp. 167-190.

Parzen, E., 1964, On statistical spectral analysis, Proc. Symp. Appl. Math., vol 26, pp. 221-246, American Math Soc., Providence.

Ross, D. T., 1954, Improved Computational Techniques for Fourier Transformation, M.I.T. Servomechanisms Lab, Cambridge.

Savit, C. H., J. T. Brustad and J. Sider, 1958, The movement filter, Geophysics, vol. 23, pp. 1-25.

Simpson, S. M., E. A. Robinson, R. A. Wiggins and C. I. Wunsch, 1963, Studies in Optimum Filtering of Single and Multiple Stochastic Processes, M.I.T., Cambridge.

Texas Instruments Staff, 1961, Vela Uniform Report.

White, J. E., 1958, Transient behavior of patterns, Geophysics, vol. 23, pp. 26-43.

Unclassified

Security Classification

DOCUMENT CONTROL DATA - R&D

(Security classification of title, body of abstract and indexing annotation must be entered when the overall report is classified)

1. ORIGINATING ACTIVITY *(Corporate author)*
Dept. of Geology and Geophysics
Massachusetts Institute of Technology
Cambridge, Massachusetts 02139

2a. REPORT SECURITY CLASSIFICATION
Unclassified

2b. GROUP

3. REPORT TITLE
SEISMIC ARRAYS FOR THE DETECTION OF NUCLEAR EXPLOSIONS

4. DESCRIPTIVE NOTES *(Type of report and inclusive dates)*
Scientific Report

5. AUTHOR(S) *(Last name, first name, initial)*
Robinson, Enders A.

6. REPORT DATE	7a. TOTAL NO. OF PAGES	7b. NO. OF REFS
June 30, 1964	107	16

8a. CONTRACT OR GRANT NO.	9a. ORIGINATOR'S REPORT NUMBER(S)
AF 19(604) 7378	Number 8
b. PROJECT NO. 8652	
c. TASK	9b. OTHER REPORT NO(S) *(Any other numbers that may be assigned this report)*
d. 865203	AFCRL - 64-855

10. AVAILABILITY/LIMITATION NOTICES
Agencies of the Department of Defense, their contractors, and Government agencies may obtain copies of this report from DDC. All others U.S. DEPT. OF COMMERCE, OFFICE OF TECH. SERVICES,

11. SUPPLEMENTARY NOTES

12. SPONSORING MILITARY ACTIVITY
Air Force Camb. Res. Labs., Office of Aerospace Research, United States Air Force, Bedford, Massachusetts

13. ABSTRACT Seismic arrays are multichannel sensor patterrns immersed in a multi-dimensional signal-noise field and the analytic problem is hence analogous to that of radar antennas. The subject is thus opened first by a review of antenna theory, considering questions of aperture width, antenna resolution, and of optimum design criteria, and secondly by a review of spectral theory, including special examination of the Ross "time gates". The general optimization problem for multichannel data leads to large systems of normal equations of Toeplitz form (as presented in previous reports) which require recursion solution techniques to be computationally feasible. Such techniques are elaborated here in terms of polynomials orthogonal on the unit circle. The specific seismic array problem is then considered in terms of plane-wave-front signal and noise contributions plus incoherent noise, and details of the "velocity filtering" method are presented. All practical array filtering rests ultimately on empirial measurements of signal and noise properties, especially of spectral behavior. Spectral estima-

DD FORM 1 JAN 64 1473

Unclassified

Security Classification

Unclassified
Security Classification

14. KEY WORDS	LINK A		LINK B		LINK C	
	ROLE	WT	ROLE	WT	ROLE	WT
Nuclear Detection						
Seismic Arrays						
Multichannel Sensor Patterns						
Antenna Theory						
Spectral Theory						
Orthogonal Polynomials						
Recursive Multichannel Computations						
Velocity Filters						
Spectral Estimations						
Aperture Functions						

INSTRUCTIONS

1. ORIGINATING ACTIVITY: Enter the name and address of the contractor, subcontractor, grantee, Department of Defense activity or other organization *(corporate author)* issuing the report.

2a. REPORT SECURITY CLASSIFICATION: Enter the overall security classification of the report. Indicate whether "Restricted Data" is included. Marking is to be in accordance with appropriate security regulations.

2b. GROUP: Automatic downgrading is specified in DoD Directive 5200.10 and Armed Forces Industrial Manual. Enter the group number. Also, when applicable, show that optional markings have been used for Group 3 and Group 4 as authorized.

3. REPORT TITLE: Enter the complete report title in all capital letters. Titles in all cases should be unclassified. If a meaningful title cannot be selected without classification, show title classification in all capitals in parenthesis immediately following the title.

4. DESCRIPTIVE NOTES: If appropriate, enter the type of report, e.g., interim, progress, summary, annual, or final. Give the inclusive dates when a specific reporting period is covered.

5. AUTHOR(S): Enter the name(s) of author(s) as shown on or in the report. Enter last name, first name, middle initial. If military, show rank and branch of service. The name of the principal author is an absolute minimum requirement.

6. REPORT DATE: Enter the date of the report as day, month, year, or month, year. If more than one date appears on the report, use date of publication.

7a. TOTAL NUMBER OF PAGES: The total page count should follow normal pagination procedures, i.e., enter the number of pages containing information.

7b. NUMBER OF REFERENCES: Enter the total number of references cited in the report.

8a. CONTRACT OR GRANT NUMBER: If appropriate, enter the applicable number of the contract or grant under which the report was written.

8b, 8c, & 8d. PROJECT NUMBER: Enter the appropriate military department identification, such as project number, subproject number, system numbers, task number, etc.

9a. ORIGINATOR'S REPORT NUMBER(S): Enter the official report number by which the document will be identified and controlled by the originating activity. This number must be unique to this report.

9b. OTHER REPORT NUMBER(S): If the report has been assigned any other report numbers *(either by the originator or by the sponsor)*, also enter this number(s).

10. AVAILABILITY/LIMITATION NOTICES: Enter any limitations on further dissemination of the report, other than those imposed by security classification, using standard statements such as:

(1) "Qualified requesters may obtain copies of this report from DDC."

(2) "Foreign announcement and dissemination of this report by DDC is not authorized."

(3) "U. S. Government agencies may obtain copies of this report directly from DDC. Other qualified DDC users shall request through _____."

(4) "U. S. military agencies may obtain copies of this report directly from DDC. Other qualified users shall request through _____."

(5) "All distribution of this report is controlled. Qualified DDC users shall request through _____."

If the report has been furnished to the Office of Technical Services, Department of Commerce, for sale to the public, indicate this fact and enter the price, if known.

11. SUPPLEMENTARY NOTES: Use for additional explanatory notes.

12. SPONSORING MILITARY ACTIVITY: Enter the name of the departmental project office or laboratory sponsoring *(paying for)* the research and development. Include address.

13. ABSTRACT: Enter an abstract giving a brief and factual summary of the document indicative of the report, even though it may also appear elsewhere in the body of the technical report. If additional space is required, a continuation sheet shall be attached.

It is highly desirable that the abstract of classified reports be unclassified. Each paragraph of the abstract shall end with an indication of the military security classification of the information in the paragraph, represented as *(TS)*, *(S)*, *(C)*, or *(U)*.

There is no limitation on the length of the abstract. However, the suggested length is from 150 to 225 words.

14. KEY WORDS: Key words are technically meaningful terms or short phrases that characterize a report and may be used as index entries for cataloging the report. Key words must be selected so that no security classification is required. Identifiers, such as equipment model designation, trade name, military project code name, geographic location, may be used as key words but will be followed by an indication of technical context. The assignment of links, rules, and weights is optional.

Unclassified
Security Classification

13. Abstract. (Continued)

tion from finite array measurements is the final question considered, including relations between continuous and discrete aperture functions, and the tabulation of aperture functions with their windows. (U)